EXPLORING THE GEOMETRY CAPTURE FEATURE IN Empipe VERSION 2.0

J.W. Bandler, S.H. Chen and N. Lin

SOS-95-R

February 1995

EXPLORING THE GEOMETRY CAPTURE FEATURE IN Empipe VERSION 2.0

J.W. Bandler, S.H. Chen and N. Lin

SOS-95-R

February 1995

EXPLORING THE GEOMETRY CAPTURE FEATURE

IN Empipe VERSION 2.0

J.W. Bandler, S.H. Chen and N. Lin

Abstract

The connection of the OSA90 [1] simulation and optimization software to the ***em*** [2] fullwave analysis software through **Empipe** [3] is an advanced idea in computer aided design. In this report we will focus on the Geometry Capture (GC) [3] technique in **Empipe**, which greatly enhances **Empipe**'s flexibility and effectiveness and makes the pipe connection more practical. The GC is examined in many aspects in this report so that its advantages are fully examined and displayed.

J.W. Bandler, S.H. Chen and N. Lin are with the Simulation Optimization Systems Research Laboratory, Department of Electrical and Computer Engineering, McMaster University, Hamilton, Ontario, Canada L8S 4L7.

J.W. Bandler and S.H. Chen are also with Optimization Systems Associates Inc., P.O. Box 8083, Dundas, Ontario, Canada L9H 5E7.

I. INTRODUCTION

Independently developed CAD software normally have unique features in different aspects. It is tempting that we take advantage of all their features at the same time for one design. This stimulates the development of inter-CAD-software interface, through which the above goal can be achieved.

From this perspective, we find that the concept of computer aided design no longer simply represents the simulation and optimization software. The kind of interfacing software mentioned above is also a constitutive part of a complete CAD package.

Interfacing is now playing a more and more important role in computer aided design. However little work has yet been done regarding the inter-CAD-software interfacing as compared to the simulation and optimization.

In this report, we attempt to do some research on the interfacing and a specific interface, **Empipe** (Here, we refer to **Empipe** 2.0) developed by the OSA inc. is discussed. Our focus is on the Geometry Capture technique which is newly built into **Empipe** for the purpose of enhancing the interface performance and effectiveness.

Before doing this, we briefly give some preparations on microstrip circuit theory and relevant CAD software.

II. MICROSTRIP CIRCUIT ANALYSIS

The microstrip circuit analysis falls into two major parts, one is the empirical analysis (less accurate), in which the closed form equations combining responses and microstrip circuit parameters are derived, the other is the full wave analysis (accurate), in which there are no direct relations between responses and microstrip circuit parameters.

A. EMPIRICAL METHOD

In the empirical method, closed form relations of responses and microstrip circuit parameters are derived from various empirical techniques. These empirical techniques include pure empirical technique (such as the trial-and-error curve fitting method) and partial empirical technique, in which, simple theoretical analysis (such as quasi-static analysis, simplified electromagnetic field analysis) are combined with data fitting equations or modified by experimental results.

Equivalent circuit method is a popular empirical method. It tries to transfer the microstrip circuit analysis to equivalent lumped circuit analysis. The equivalent circuits of conventional microstrip elements have been intensively studied [4] [5]. They are either T-network or Π-network (shown in Fig. 1) of lumped element Y_n or Z_n (except for microstrip line). The expressions of the lumped elements Y_n or Z_n in terms of microstrip circuit parameters [4] [5] are found using empirical techniques. After the expressions are obtained, we can apply traditional circuit and network analysis to characterize the original microstrip circuit.

The equivalent circuit idea itself and the empirical technique employed are not quite accurate. However the equivalent circuit is descriptive and helpful in the understanding of the function of the real microstrip structure. Also, Since the closed form equations are available, it demands little computation for solution.

B. FULLWAVE METHOD

The full wave analysis methods is a method developed specifically to deal with the microwave circuits. ~~In this method~~, Maxwell's equations are directly applied, manipulated and solved according to boundary conditions.

The Method of Moments [6] is a fullwave method, which is applicable to microwave structures of arbitrary geometry and arbitrary material. ~~In this method~~, field equations are reduced to matrix equations. The name Method of Moments implies the mathematical procedure for obtaining the matrix equations. This method gives a general procedure for treating field problems,

but the solution method varies widely with the particular problem. The solution method, employed by ***em***, is suitable for microstrip structures and is easy to be built into CAD. This will be discussed in detail in Section III. B.

Since the electromagnetic field is precisely analyzed, this method offers high accuracy, and further, the electromagnetic analysis provides a great physical insight. However, it demands huge computation for solution.

III. SOFTWARE INTRODUCTION

A. OSA90 OVERVIEW

OSA90 [1] is an advanced CAD software system. It provides linear and nonlinear circuit simulation and noticeably a large variety of powerful, state-of-the-art optimizers with proven track records. All the advanced optimizers are built into the OSA90. They are

(1) gradient-based minimax optimizer

(2) gradient-based l_1 optimizer

(3) gradient-based l_2 optimizer

(4) gradient-based quasi-Newton optimizer

(5) conjugate-gradient optimizer

(6) Huber optimizer

(7) non-gradient simplex optimizer

(8) random optimizer

(9) robust gradient-based yield optimizer.

Using these powerful tools, users can optimize circuit responses (DC, small-signal AC and large-signal), postprocessed responses, mathematical expressions, and functions calculated by external simulators connected via datapipe.

B. *em* OVERVIEW

em [2] is a software package that performs fullwave analysis on planar waveguiding structures using the Method of Moments. The *em* simulation process is outlined below.

(1) *em* reads two inputs, one, the ASCII ".geo" file (created by ***xgeom*** [7]) describing the planar waveguiding circuit; the other, the ASCII ".an" file specifying the simulation frequency.

(2) *em* subsections the circuit using variable size subsections (the upper and lower limits of the subsection size are defined in the ".geo" file) so that small subsections are used where the field changes sharply, and large subsections are used where the field changes smoothly. This is done transparently to the user.

(3) *em* calculates the *S* parameter of the circuit.

(i) To start with, *em* assumes the currents on all the subsections.

(ii) *em* evaluates the electric field everywhere due to the current in a single subsection (coupling calculation), and *em* does the same evaluation for all the subsections.

(iii) *em* sums up the electric field produced by all the subsections.

(iv) *em* adjusts the currents in each subsection, repeats (ii) and (iii), until the total tangential electric field goes to 0 wherever there is conductor. The currents that do this form the current distribution on the circuit metallization.

(v) *em* calculates the *S* parameter of the circuit from the current distribution. Then outputs the circuit's *S* parameters to an ASCII ".rsp" file.

(vi) *em* repeats (i) to (v) for each frequency specified in ".an" file.

The unique feature of the *em* simulation is its high accuracy. There are two main approximations used by *em*,

(1) *em* subdivides the metallization into small subsections.

(2) The coupling between subsections is an infinite summation which *em* truncates.

The two approximations may cause inaccurate results especially for approximation (1). When subsection size is allowed to change widely, circulate current may occasionally be generated

at the interface of several widely varied subsections. The circulate current is caused by the improper subsection at the regarding location and does not represent the real current distribution. This may cause significant error in the S parameter.

Fortunately, ***em*** gives the user full control over these approximations so that ***em*** results can reach high accuracy (the results can be accurate to within 0.1%). When the dynamic range of the subsection size is decreased, the occurrence of circulate current will be quickly decreased. However, the cost of this is the more ***em*** time. It is the user's discretion to balance between time and accuracy. In our future discussion, the maximum subsection size is set to 20 per wavelength, the minimum subsection size is set to the cell size. This settings have been tested reasonable.

C. **Empipe** OVERVIEW

OSA90 has been successfully connected to ***em*** through the **Empipe** [3]. Through this connection, OSA90's powerful optimization and ***em***'s accurate microstrip analysis can be used jointly in microstrip circuit design.

Empipe is a much advanced interprocess pipe (based on the General Purpose Modelling Interface (GPMI) [8]) in that it provides

(1) a library of preprogrammed (hard copy), ***em***-ready components. These components, on the one hand, can be referred to in the OSA90 circuit file just like any other OSA90 elements, on the other hand, are ready to input into ***em***. This makes ***em*** and OSA90 seamlessly connected.

(2) Unified interpolation/modelling technique aiming at saving the expensive ***em*** simulations.

(3) Database subsystem which saves previous ***em*** simulation results for future use.

(4) Parallel processing subsystem.

Further, through the built-in Geometry Capture, some more features are added to the **Empipe**.

(1) Through GC, user is enabled to generate ***em***-ready elements. This makes it possible to treat a complex microstrip planar structure as a single element, in stead of having to decompose it into several ***em*** library elements. The decomposition may reduce the accuracy, since the library elements are connected by the circuit-level simulator.

(2) Simulation grid and response modelling grid can now be defined separately to maximally adapt different simulation and modelling situations. We can define the modelling grid size multiple of the simulation grid size in the case when accurate simulation result is required, while the response curve is well behaved over a large region in which quadratic interpolation can be effective. This helps to save the expensive ***em*** simulations.

(3) A benefit of the separation of the simulation and modelling grids is that parameter discretization (for modelling) can be extended beyond the few discretized simulation parameters (i.e. geometry parameters) in the library elements. Other parameters, such as the substrate height, substrate dielectric constant, etc., can all be discretized for modelling. When optimization or sweeping of these parameters are required, lots of ***em*** simulations will be saved through interpolations.

(4) Combination of several design parameters into one and implication of constraints on parameters are possible through GC. This makes the selection and definition of design parameter more flexible and helps better representing the engineering requirements.

(5) DC *S* parameter obtained from other processes is accepted into **Empipe** to combine with the ***em***'s AC *S* parameter. This complements the absence of ***em***'s DC analysis. Since there are sophisticated DC analysis methods (static analysis methods), normally, the DC *S* parameters are no less accurate than the ***em*** results. The combined results are equally as accurate as before.

We will apply the user defined element (UDE) to simulate several microstrip elements. For different elements, we focus on examining different aspects of the UDE simulation approach, and

always compare its results with the library element (LE) simulation results. The results are all presented in the form of S parameter. The notation $|S_{mn}|$ represents the magnitude of S_{mn} and θ_{mn} represents the phase of S_{mn}.

IV. ELEMENT 1: MICROSTRIP ASYMMETRICAL GAP

For this element, we focus on the error between the UDE simulation results and the LE simulation results for on-grid and off-grid points.

The structure of the microstrip asymmetrical gap is shown in Fig. 2 (a).

For the microstrip asymmetrical gap library element **EM_AGAP**, all the parameters (Geometry, Substrate and Control parameters [3]) are inherently set as design parameters. The parameters are either discretized in the sense of both simulation and modelling (parameters W_1, W_2 and S) or continuous (parameters other than W_1, W_2 and S).

For the microwave asymmetrical gap user defined element **AGAP**, we define W_1, W_2, S as design parameter, and the other parameters as non-design parameters. We generate a set of ".geo" files (through ***xgeom***) for the **Empipe** to capture the design parameters and non-design parameters. The set of ".geo" files and their representing structures are shown in Fig. 3.

All the above information necessary for the capturing of **AGAP** are passed into **Empipe** through the *em parameterization* window (shown in Fig. 6).

After parameterization, the user defined ***em*** element **AGAP** with 3 design parameters is created in the file "agap.inc" (shown in Appendix B).

In the UDE approach, it is up to the user to limit the number and type of design parameters due to practical requirements. All the non-design parameters are set to constant in the include file. Here, for the **AGAP**, we set

Substrate thickness H = 10 mil
Relative dielectric constant ε_r = 9.9

Cell size $\begin{cases} X_{CELL} = 2 \text{ mil} \\ Y_{CELL} = 2 \text{ mil} \end{cases}$

Simulation frequency $\begin{cases} f_{\min} = 5 \text{ GHz} \\ f_{\max} = 20 \text{ GHz} \\ f_{step} = 1 \text{ GHz} \end{cases}$

Substrate box marginal spacing normalized w.r.t. H $\begin{cases} LEFT = 5.8 \\ RIGHT = 5.8 \\ TOP = 4.6 \\ BOTTOM = 4.6 \end{cases}$

The remaining non-design parameters are set to the default values of the corresponding library element **EM_AGAP**.

Now we write an OSA90 circuit file to compare the **AGAP** and **EM_AGAP** simulation results for an asymmetrical microstrip gap. Be sure that same parameter values are set to the two elements.

(1) On-Grid Point simulation.

Perform on-grid simulation with the simulation point p_1 selected as

$$W_1 = 16 \text{ mil}$$
$$W_2 = 28 \text{ mil}$$
$$S = 4 \text{ mil}$$

The circuit file are shown in Appendix A.

The geometry files generated by **AGAP** and **EM_AGAP** are also shown in Appendix A. Except for different version (style), the two geometry files represent the same microstrip structure. The difference in the definition of the polygons is due to the different sequence of each vertices being defined.

The simulation results at p_1 from the two approaches are compared in Table I. The error between the two approaches are also presented in this table, where the error is defined as

$$E_{|S|} = \frac{||S|_{(UDE)} - |S|_{(LE)}|}{|S|_{(UDE)}} \times \%$$

$$E_{\theta} = \frac{|\theta_{(UDE)} - \theta_{(LE)}|}{|\theta_{(UDE)}|} \times \%$$

From the table, we find that except for some very slight difference, the two responses are the same. The difference is due to the ***em*** approximations discussed in section **III.B.** and can be ignored.

The curves of $|S_{11}|$, $|S_{12}|$ and $E_{|S|}$, E_{θ} at p_1 are shown in Fig. 7. We can see that $|S_{11}|_{(UDE)}$ and $|S_{11}|_{(LE)}$, $|S_{12}|_{(UDE)}$ and $|S_{12}|_{(LE)}$ are completely overlapped.

The UDE approach for on-grid simulation is valid, it provides the same results as the LE approach.

(2) Off-grid simulation

The simulation of the off-grid point is performed in **Empipe** through three steps

Step 1: on-grid snapping.

Step 2: on-grid simulation.

Step 3: interpolation.

For the step 2, we have verified above that the UDE and LE approach give same results. However, for step 1 and 3, the UDE and LE approach give or may give slightly different results. This is detailed below.

Case 1 Off-grid point is not in the middle of two grids.

We select the simulation point p_2 as

W_1 = 19.7 mil
W_2 = 31.6 mil
S = 4.3 mil

After running the circuit file, **Empipe** snaps this off-grid points to 4 on-grid point and hence 4 geometry files are generated respectively in UDE and LE approach. The geometry files (empl_11.geo.*n*) in LE approach are correspondent to the geometry files (agap_1.in.*n*) in the UDE approach. The correspondence is shown in Table II.

The arrows in Table II indicates the identical geometry file pairs, i.e. each pair represents same microstrip structure, just like the two identical ".geo" files generated at point p_1.

Thus, in the case when off-grid point is not at the middle of two grids, step 1 (snapping) in the UDE and LE approach gives same results.

However, for step 3 (interpolation), there exists difference between the UDE approach and LE approach. In the UDE approach, interpolation is performed on the real and imaginary part of the S parameter respectively, while in the LE approach, interpolation is performed on the magnitude and phase respectively. This difference may cause slightly different interpolation results.

The simulation results at p_2 from the two approaches are compared in Table III. The error is larger than that in the on-grid case. This is mainly due to the different interpolation methods.

The curves of $|S_{11}|$, $|S_{12}|$ and $E_{|S|}$, E_θ at p_2 are shown in Fig. 8. We can see that $|S_{11}|_{(\text{UDE})}$ and $|S_{11}|_{(\text{LE})}$, $|S_{12}|_{(\text{UDE})}$ and $|S_{12}|_{(\text{LE})}$ are overlapped quite well. The difference caused by the interpolation can be ignored. Both interpolation methods are valid.

Case 2 Off-grid point is in the middle of two grids.

We select the simulation point p_3 as

$$W_1 = 19 \text{ mil}$$
$$W_2 = 30 \text{ mil}$$
$$S = 3 \text{ mil}$$

This time, the geometry files generated in each approach are not correspondent to each other (Table IV). This is because that the nominal snapping point is selected differently, and hence the 4 snapping points are different in the each approach.

Thus, in the case when off-grid point is at the middle of two grids, Step 1 gives different results. We find that, when a point is at the center of two grids, in the UDE approach, the higher value grid is selected as the nominal point, while in the LE approach, the lower value grid is selected as the nominal point. This causes the different geometry files shown in Table IV.

The simulation results from the two approaches are compared in Table V.

The error between the two results are larger than before. This is caused by the difference in Step 1 snapping and Step 3 interpolation.

The curves of $|S_{11}|$, $|S_{12}|$ and $E_{|S|}$, E_θ at p_3 are shown in Fig. 9. We can see that $|S_{11}|_{(\mathrm{UDE})}$ and $|S_{11}|_{(\mathrm{LE})}$, $|S_{12}|_{(\mathrm{UDE})}$ and $|S_{12}|_{(\mathrm{LE})}$ are overlapped not so well. Since the snapping and interpolation methods in both approaches are reasonable, both UDE and LE results are valid in this case.

V. ELEMENT 2: MITERED MICROSTRIP BEND

For this element, we focus on the new feature in the UDE approach that nongeometrical parameter can be discretized for the purpose of modelling.

In the UDE approach, when a parameter is defined as a design parameter, it is automatically discretized in the *em parameterization window* for modelling. Thus, any kind of parameter is possible to be discretized for modelling.

The structure of the metered microstrip bend is shown in Fig.1 (b).

For the mitered microstrip bend library element **EM_BEND2**, all the microstrip parameters are design parameters, in which, the parameter W_1, W_2, L_1 and L_2 are discretized for simulation and modelling, the others are continuous parameters.

For the mitered microstrip bend user defined element **BENDM**, we define the design parameter as: W_1, W_2, L_1, L_2 and ε_r . Then ε_r is discretized for interpolation (modelling), while the other four are discretized for simulation and interpolation. When we sweep or optimize the ε_r to select a proper dielectric constant, a lot of ***em*** time will be saved through interpolations.

Going through the same procedure as before, the user defined ***em*** element **BENDM** with 5 design parameters is created in the "bendm.inc" (The parameterization portion of this include file is shown in Appendix B).

Now we compare the **BENDM** and **EM_BEND** simulation results on a mitered microstrip bend at point p_4

W_1 = 32 mil	on-grid for UDE and LE
W_2 = 32 mil	on-grid for UDE and LE
L_1 = 22 mil	on-grid for UDE and LE
L_2 = 22 mil	on-grid for UDE and LE
ε_r = 9.83	off-grid for UDE

We now examine the error between the results from the UDE approach where interpolation is invoked to simulate the off-grid ε_r, and the results from the LE approach where direct simulation on the ε_r is performed.

Empipe snaps the off-grid point to 2 on-grid points (32, 32, 22, 22, 9.8) and (32, 32, 22, 22, 9.9) in UDE approach, and in the LE approach, since the point is already on-grid, no snapping is needed.

The simulation results from the two approaches are compared in Table VI.

There exist some slight differences between the two results since the LE results (without interpolation on ε_r) are a little more accurate than the UDE results.

The curves of $|S_{11}|$, $|S_{12}|$ and $E_{|S|}$, E_θ at p_4 are shown in Fig. 10. We can see that $|S_{11}|_{(\mathrm{UDE})}$ and $|S_{11}|_{(\mathrm{LE})}$, $|S_{12}|_{(\mathrm{UDE})}$ and $|S_{12}|_{(\mathrm{LE})}$ are overlapped quite well. The error introduced by the interpolation in the UDE approach can be ignored. The UDE approach is valid in this case.

VI. ELEMENT 3: MICROSTRIP DOUBLE PATCH CAPACITOR

For this element, we will examine the error between UDE results and LE results for wider frequency range.

The structure of the double patch microstrip capacitor is shown in Fig. 2 (c).

We create an user defined double patch capacitor **DPCAP** in the "dpcap.inc" (The parameterization portion of this include file is shown in Appendix B). For this element L_1, L_2, S, W_1, W_2 and W_3 are defined as design parameters, and the frequency range is broadened from 0.5 GHz to 49.5 GHz (***em*** can not simulate DC circuit).

For the user defined element, the selection of the frequency step in the include file has some effects on the empipe. We find that when f_{step} is selected such that

$$f_{max} - f_{min} \neq n \times f_{step} \qquad n = 1,2,3,...$$

the empipe breaks just before transferring the simulation data back to OSA90.

For example, when f_{step} is set to 2.0 GHz in the "dpcap.inc", simulation on **DPCAP** goes on quite well from 0.5 GHz, 2.5 GHz,..., 48.5 GHz. After the simulation on 48.5 GHz, the child terminates, giving the message 'Wrong format of the ".raw" file' since the sweeping frequency set can not cover the f_{max} frequency (49.5 GHz).

On the other hand, for the library element, there is no problem with the same frequency settings. After the child program simulating all the frequency (0.5 GHz, 2.5 GHz,..., 48.5 GHz), it transfers the results to OSA90.

Now we simulate the double patch capacitor at an on-grid point p_5

$$\begin{aligned} W_1 &= 24 \text{ mil} \\ W_2 &= 64 \text{ mil} \\ W_3 &= 16 \text{ mil} \\ L_1 &= 26 \text{ mil} \\ L_2 &= 30 \text{ mil} \\ S &= 6 \text{ mil} \end{aligned}$$

through UDE approach and LE approach. Be sure to set all the parameters to same values for both elements (f_{step} is set to 1.0 GHz).

The simulation results from the two approaches are compared in Table VII and Fig. 11. The very slight differences between the two results is due to ***em*** approximation and can be ignored. The UDE approach is valid for wide range frequency simulation.

VII. ELEMENT 4: MICROSTRIP LINE

Our previous simulations are all performed with de-embedding. Through de-embedding, ***em*** removes from the results

(1) port discontinuities.

(2) connecting transmission line between the port and the element (reference plane shift).

With de-embedding, more accurate S parameter values of the regarding element are obtained.

Since in the UDE approach, users, by modifying the include file, can select between de-embedding or non de-embedding (for the library elements, de-embedding is inherently set), we can now compare the ***em*** non de-embedding simulation results and de-embedding simulation results to have an idea of the effects of port discontinuity and connecting microstrip line on the S parameters.

The structure of the microstrip transmission line is shown in Fig. 2 (d). Since there is no reference plane, ***em*** non-de-embedding results will be only affected by the port discontinuity.

We create an user defined microstrip line de-embedding model **ML** in "ml.inc" (The parameterization portion of this include file is shown in Appendix B), and non-de-embedding model **MLND** in "mlnd.inc", in both of which, L and W are design parameters.

Now we simulate a microstrip line at an on-grid point p_6

$$W = 20 \text{ mil}$$
$$L = 120 \text{ mil}$$

using **ML** and **MLND**.

The simulation results of $|S_{11}|$ and $|S_{12}|$ are compared in Fig. 12 (f). We find that port discontinuities have a significant influence on the simulation results.

VIII. ELEMENT 5: ASYMMETRICAL MICROSTRIP DOUBLE STUB

For this element, we will focus on the UDE feature of separate simulation and modelling grid definition.

The structure of the stub is shown in Fig. 2 (e). As mentioned before, for UDE, when a response curve changes smoothly with certain geometrical parameter, modelling grid size for this parameter can be multiples of its simulation grid size (For library element, the two sizes are always the same). Interpolation saves the ***em*** simulations.

We create an user defined double stub **DSTB** in the "dstb.inc" (The parameterization portion of this include file is shown in Appendix B). For this element L_1, L_2, L_3, W_2 and W_3 are design parameters. The modelling grid size is same as their simulation grid size for L_1, W_2 and W_3 while twice their simulation grid size for L_2 and L_3.

On the other hand, for the corresponding library element, we define the cell size (which means both the simulation and modelling grid size) same as the UDE simulation grid size (2 mil).

Now we compare the UDE and LE results of same simulation grid size, different modelling grid size at a point p_7

$$
\begin{aligned}
W_2 &= 20 \text{ mil} \\
W_3 &= 16 \text{ mil} \\
L_1 &= 34 \text{ mil} \\
L_2 &= 42 \text{ mil} \\
L_3 &= 40 \text{ mil}
\end{aligned}
$$

At this point, interpolation is invoked in the UDE approach, while direct simulation is performed in the LE approach.

The simulation results on $|S_{11}|$, $|S_{12}|$ and $E_{|S|}$ from the two approaches are compared in Fig. 13. The error introduced into the UDE interpolated responses is acceptable. The separate definition of the simulation and modelling grid size is feasible.

IX. ELEMENT 6: MICROSTRIP RECTANGULAR STRUCTURE

In the UDE approach, GC allows user to combine several parameters into one and express graphically subtle constraints in the geometrical structure through ***xgeom***, which are otherwise complicated or difficult to define.

For this element, we will examine this Implicit Definition feature and show its advantages.

The structure of the rectangular is shown in Fig. 2 (f).

In the UDE approach, in stead of defining the rectangular using W_2 and L two parameters, we define a scaling parameter S, which implies the changing of the W_2 and L proportionally at the same time, i.e.

$$S = 4 \text{ implies } \begin{matrix} L = 40 \text{ mil} \\ W_2 = 48 \text{ mil} \end{matrix}$$

$$S = 5 \text{ implies } \begin{matrix} L = 50 \text{ mil} \\ W_2 = 60 \text{ mil} \end{matrix}$$

$$S = 6 \text{ implies } \begin{matrix} L = 60 \text{ mil} \\ W_2 = 72 \text{ mil} \end{matrix}$$

The user defined rectangular **RECS** with 3 design parameters S, W_1 and W_2 is created in "recs.inc" (The parameterization portion of this include file is shown in Appendix B). The 4 geometrical structures for capturing **RECS** are shown in Fig. 4.

Now we simulate a rectangular structure at an on-grid point p_8

$$\begin{matrix} S = 6 \\ W_1 = 16 \text{ mil} \\ W_3 = 20 \text{ mil} \end{matrix}$$

through UDE and LE approach respectively.

The simulation results are compared in Table VIII and Fig. 14. The two results are the same. The implicit definition method is valid and efficient.

X. ELEMENT 7: MICROSTRIP INTERDIGITAL CAPACITOR

In the previous definition of UDE element, we define structures using the same polygon group (indicated in each structure shown in Fig. 2) as that is used for the corresponding library elements.

Now, for this element (structure shown in Fig. 2 (g)), we define the UDE **DCAP** using 2 polygon (also indicated in Fig. 2 (g)), while for the library interdigital capacitor **EM_DCAP**, 5 polygons are used (see [3]). Theoretically, the two kinds of definitions are identical. However, because ***em*** subsection may be different in different cases, the ***em*** simulation results on **DCAP** and **EM_DCAP** may be different. This will be shown later on.

Originally, we define 4 design parameters W, G, L and S. considering of the fact that, the change of W is for the accommodating of the change of G, and the change of S is for the accommodating of the change of L, we can apply implicit definition on W and S. In the ".geo" file that defines G, we also change W accordingly to maintain the same structure shape, and in the ".geo" file that defines L, we also change S accordingly so that $(S-L)$ remains constant. In this way, parameter W and S can be spared. The 3 ".geo" structures for capturing **DCAP** are shown in Fig. 5.

Now we simulate an interdigital capacitor at a on-grid point p_9

$$L = 66 \text{ mil}$$
$$G = 6 \text{ mil}$$

using the **DCAP** and **EM_DCAP** respectively to have an idea of the effect of different polygon definition on the results.

The results from the UDE approach and LE approach are compared in Table IX and Fig 15. We find that, the different polygon group definition causes different results. The error reaches 28% in the worst case. Further examine the response files, we find that, in the 2 polygon definition approach, the capacitor is subsectioned into 288 sections, while, in the 5 polygon

definition approach, the capacitor is subsectioned into 264 sections. This is the cause of the different simulation results. The explanation for this is stated below.

When the structure is divided into rectangular polygons, ***em*** subsections each rectangular separately. When the structure is defined using one polygon, ***em*** subsections the structure as a whole. The subsection is more accurate at the cross rectangular regions when the structure is defined as one polygon. Whereas, when the structure is defined as several rectangular polygons, the subsection is confined by the rectangular boundary at the cross rectangular regions and these region can not be subsectioned as an integral part.

Thus the UDE results is more accurate than the LE results in this case. We should use as few polygons as possible when we create user defined elements.

XI. ELEMENT 8: MICROSTRIP OVERLAY DOUBLE PATCH CAPACITOR

The structure of this capacitor is shown in Fig. 2 (h). It is a multilayer microstrip structure. We will now examine the error between the UDE approach and LE approach for the multilayer microstrip structure.

Since we have found that defining consecutive structure using one polygon gives more accurate results, now for the user defined structure **ODPC**, we define the capacitor in this way. The **ODPC** include file with design parameter W_1, W_2, W_3, L_1, L_2 and S is created in "odpc.inc" (The parameterization portion of this include file is shown in Appendix B).

Now we simulate an overlay double patch capacitor at an on-grid point p_{10}

$$
\begin{aligned}
W_1 &= 16 \text{ mil} \\
W_2 &= 48 \text{ mil} \\
W_3 &= 36 \text{ mil} \\
L_1 &= 22 \text{ mil} \\
L_3 &= 24 \text{ mil} \\
S &= 4 \text{ mil}
\end{aligned}
$$

using UDE and LE approach respectively.

The simulation results are compared in Table X and Fig. 16. The two results are almost the same. The difference is mainly caused by different polygon group definitions. The UDE approach is valid for multilayer microstrip structure.

XII. ELEMENT 9: MICROSTRIP OPEN STUB

In the previous definition of UDE, the materials, metallization and dielectric, are all assumed lossless. In the lossless case, we have verified that the UDE results are same or even better than the LE results.

Now, for this element, we will test the UDE approach for lossy materials and compare the UDS and LE lossy results.

There are two kinds of loss, the dielectric loss and the metallization loss. For microstrip circuits, the dielectric loss is, in general, very small compared to the conductor loss at microwave frequency [4].

The ways of definition of microstrip loss are different in the UDE and LE approach. In the LE approach, the definition follows OSA90 convention, while in the UDE approach, the definition follows the ***xgeom*** convention. The loss parameters defined in the LE approach and UDE approach are compared in Table XI. In this table, the relationship between the two sets of loss parameters are also given.

Now we create an user defined structure **OPE** in "ope.inc" (The parameterization portion of this include file is shown in Appendix B). For this element, L and W are design parameters, and the lossy parameters are set as

(1) Dielectric loss

$$\tan\delta = 0.001$$

(2) Metallization loss

$$R_{DC} = 0.0013543\ (\Omega/\mathrm{m}^2)$$

$$X_{DC} = 0$$

$$R_{RF} = 2.60582 \times 10^{-7}\ (\Omega\ \mathrm{Hz}^{-1/2}/\mathrm{m}^2)$$

Now, we simulate a lossy microstrip open stub at point p_{11}

$$W = 20\ \text{mil}$$
$$L = 60\ \text{mil}$$

through UDE approach and LE approach. To ensure the same lossy condition, the loss parameters defined in the UDE approach is translated into the loss parameters in the LE approach through the relations in Table XI. After transformation, we obtain

(1) Dielectric loss

$$\tan\delta = 0.001$$

(2) Metallization loss

$$\rho_c = 1.7200025 \times 10^{-8}\ (\Omega/\mathrm{m}^3)$$

$$X_S = 0$$

It takes more time for ***em*** to simulate a lossy structure because the ***em*** computation becomes complex. The simulation results are compared in Table XII and Fig. 17. The error is caused by

(1) the ***em*** approximation,

(2) the approximation introduced during the loss parameters conversion between UDE and LE.

The two errors are very small and can be ignored.

Thus we conclude that, in the lossy case, UDE approach is equally as effective as the lossless case.

XIII. ELEMENT 10: MICROSTRIP DOUBLE FOLDED STUB

We have now discovered that the Geometry Capture technique greatly increased the capability of **Empipe**. Though GC, ***em*** simulation and optimization become more flexible and adjustable and the number and time of ***em*** simulations are reduced wherever possible. We now try to solve a more practical problem using the Geometry Capture technique.

We will optimize a double folded stub microstrip filter according to the specification

pass band: $|S_{21}| \geq -3$ for 5 GHz $\leq f \leq$ 9.8 GHz and 17 GHz $\leq f \leq$ 20 GHz

stop band: $|S_{21}| \leq -25$ for 12.2 GHz $\leq f \leq$ 14.8 GHz

The structure of this filter is shown in Fig. 2 (j). The optimizable parameters are L_1, L_2, L_3, S_1 and S_2. The other geometry and non-geometry parameters are all set before hand, i.e.

$$W_1 = W_2 = W_3 = 4.8 \text{ mil}$$

Substrate thickness $H = 5$ mil
Relative dielectric constant $\varepsilon_r = 9.9$

Cell size $\begin{cases} X_{CELL} = 2 \text{ mil} \\ Y_{CELL} = 2 \text{ mil} \end{cases}$

Simulation frequency $\begin{cases} f_{min} = 5 \text{ GHz} \\ f_{max} = 20 \text{ GHz} \\ f_{step} = 0.25 \text{ GHz} \end{cases}$

Substrate box marginal spacing normalized w.r.t. H $\begin{cases} LEFT = 8.0 \\ RIGHT = 8.0 \\ TOP = 6.4 \\ BOTTOM = 6.4 \end{cases}$

The starting point p_s is

$L_1 = 84$ mil
$L_2 = 80$ mil
$L_3 = 80$ mil
$S_1 = 4.8$ mil
$S_2 = 4.8$ mil

We assume that this point is the design result of a previously designed filter with higher stop band than the specification. The taking of previous design result as a starting point speeds our new design and makes the design problem simpler.

Now, we perform ***em*** simulation and OSA90 optimization through **Empipe**. Same as before, we will compare the UDE and LE approach in the process.

First, we create an user defined element **FDST** according to the above requirements. Conventionally, we define optimizable parameter L_1, L_2, L_3, S_1 and S_2 as design parameter. However, in this case, the non-design parameter W_1, W_2 and W_3 are off-grid. Off-grid point can only be simulated through interpolation. This requires that W_1, W_2 and W_3 be also defined as a variable (i.e. design parameter).

In the definition of **FDST**, we apply the following three GC advanced features to improve ***em*** simulation efficiency and accuracy.

(1) Define the filter with one polygon which increases the ***em*** analysis accuracy without increasing ***em*** simulation time.

(2) Since W_1, W_2 and W_3 are set to the same off-grid value, it is not necessary for the three parameters to be changed individually. We implicitly define them as one parameter W so that they always change simultaneously. In this way, the number of the design parameters is reduced by 2. The number of snapping point will also be reduced by 2 (at most 7 snapping points) and the off-grid simulation will be sped up without losing accuracy.

(3) Since the responses are more sensitive to the change of width than the change of length, the modelling (interpolation) grid for length can be larger than for width. Here, we define the modelling grid for L_2 and L_3 the twice the simulation grid size (or the cell size), and for the other parameters the same as the simulation grid size. In this way, the optimization will be sped up (especially during multiple iterations) without losing much accuracy.

The include file "fdst.inc" incorporated with these features is partly shown in Appendix B.

For the corresponding library element **EM_FDST2**, there is not so much flexibility.

(1) The structure is defined with 3 polygons. This may cause the ***em*** analysis at the cross polygon region inaccurate.

(2) All the 8 geometry parameters W_1, W_2, W_3, L_1, L_2, L_3, S_1 and S_2 should be snapped individually during interpolation. Hence at most 9 snapping point will be created.

(3) For the **EM_FDST2**, the simulation grid and the modelling grid are always the same as the cell size. ***em*** will be more frequently evoked during optimization.

Now, we optimize the filter with the UDE **FDST** and LE **EM_FDST2** respectively from starting point p_s. The simulation results before optimization from the two approaches are compared in Fig. 18 (a). We find that, the UDE simulation, by taking advantage of the GC features, is faster than the LE simulation (detailed in Table XIII) without losing accuracy (in Fig. 18 (a), $|S_{21}|_{(\mathrm{UDE})}$ and $|S_{21}|_{(\mathrm{LE})}$ are almost overlapped).

Perform minimax optimization on **FDST** and **EM_FDST2** under same conditions. Similar optimal points are obtained (see Table XIII). Both optimums satisfy the specification (see Fig. 18 (b)). However, UDE optimization is even more faster than the LE optimization. Under same CPU percentage (around 25%) , the LE takes around 5 days, while the UDE takes only around 1 day. These are all detailed in Table XIII. The saving of ***em*** simulations is more obvious during optimization than simulation.

One thing we should mention. The number of the iterations may not be equal in the two approach. This is because that the objective functions are slightly different due to the GC techniques employed in UDE approach. However, even the UDE optimization goes through more iterations than the LE optimization, we find usually UDE approach is still much faster. This is because, in gradient-based optimization, search points (except for first several ones) tends to gather around the optimum. new ***em*** simulation are less frequently evoked, and interpolations are more

frequently performed with the optimization goes on. The iterations will become faster and faster. In both approach, the ***em*** optimization time is mainly spent on the first several iterations.

Now, we conclude that fully taking advantage of Geometry Capture makes the simulation and optimization process more efficient without losing ***em*** accuracy.

XIV. CONCLUSION

The connection of OSA90 software to ***em*** through **Empipe** suggested a new area for computer aided engineering. With advanced datapipes, various CAD software can be integrated into one powerful comprehensive package for future high standard simulation and optimization.

In this report, the Geometry Capture of **Empipe** is discussed and tested from various perspectives. We find that GC is the essence of the **Empipe** version 2.0. With it, this inter-CAD-software interface becomes more flexible and effective.

From the experience and knowledge gained in the above work, the authors suggest some future research directions.

(1) Further work is needed for further exploring and exploiting the GC technique. We even speculate that, by fully taking advantage of the GC, some ***em*** defects may be removed (such as the circulate current problem).

(2) In Section **XIII**, we only give a preliminary discussion on optimization. However, optimization through GC is a big subject that more efforts should be put into.

The authors is presently doing research in these directions and will present more confident results in the future.

XV. REFERENCE

[1] *OSA90/hope*, Optimization Systems Associates Inc., P.O. Box 8083, Dundas, Ontario, Canada L9H 5E7, 1993.

[2] ***em***, Sonnet Software, inc., 135 Old Cove Road, Suite 203, Liverpool, NY 13090-3774, May, 1992.

[3] **Empipe**, Optimization Systems Associates Inc., P.O. Box 8083, Dundas, Ontario, Canada L9H 5E7, 1993.

[4] K.C. Gupta, R. Garg and R. Chadha, *Computer-Aided Design of Microwave Circuit*, Artech House, Inc., 610 Washington Street, Dedham, MA, 1981.

[5] I. Bahl and P. Bhartia, *Microwave Solid State Circuit Design*, John Wiley & Sons, Inc., New York, 1988.

[6] R.F. Harrington, "Matrix Methods for Field Problems", *Proceedings of the IEEE*, vol. 55, no. 2, pp. 136-149.

[7] ***xgeom***, Sonnet Software, inc., 135 Old Cove Road, Suite 203, Liverpool, NY 13090-3774, May, 1992.

[8] Piotr A. Grobelny, *Integrated Numerical Modeling Techniques For Large Scale Nominal And Statistical Circuit Design*, Ph.D. dissertation (in preparation), Department of Electrical and Computer Engineering, McMaster University, Hamilton, Ontario, 1995.

TABLE I

SIMULATION RESULTS FOR AN ASYMMETRICAL MICROSTRIP GAP AT p_1 (ON-GRID) FROM THE UDE AND LE APPROACH

f (GHz)	$\lvert S_{11}\rvert$	$\lvert S_{12}\rvert$	$\lvert S_{21}\rvert$	$\lvert S_{22}\rvert$	θ_{11}	θ_{12}	θ_{21}	θ_{22}
(Results from the UDE approach)								
5	0.9982	0.06029	0.06029	0.9982	-4.61	84.31	84.31	-6.78
6	0.9974	0.07188	0.07188	0.9974	-5.514	83.2	83.2	-8.09
7	0.9965	0.08322	0.08322	0.9965	-6.41	82.1	82.1	-9.401
8	0.9955	0.09427	0.09427	0.9955	-7.296	81.01	81.01	-10.69
9	0.9945	0.105	0.105	0.9945	-8.17	79.93	79.93	-11.96
10	0.9933	0.1154	0.1154	0.9933	-9.034	78.88	78.88	-13.21
11	0.9921	0.1255	0.1255	0.9921	-9.886	77.84	77.84	-14.43
12	0.9908	0.1352	0.1352	0.9908	-10.72	76.82	76.82	-15.63
13	0.9895	0.1445	0.1445	0.9895	-11.55	75.82	75.82	-16.81
14	0.9881	0.1535	0.1535	0.9881	-12.35	74.85	74.85	-17.95
15	0.9868	0.1621	0.1621	0.9868	-13.15	73.89	73.89	-19.07
16	0.9854	0.1703	0.1703	0.9854	-13.93	72.95	72.95	-20.16
17	0.984	0.1782	0.1782	0.984	-14.7	72.04	72.04	-21.23
18	0.9826	0.1858	0.1858	0.9826	-15.45	71.14	71.14	-22.27
19	0.9812	0.1931	0.1931	0.9812	-16.19	70.26	70.26	-23.29
20	0.9798	0.2001	0.2001	0.9798	-16.92	69.39	69.39	-24.29
(Results from the LE approach)								
5	0.9982	0.06029	0.06029	0.9982	-4.61	84.3	84.3	-6.78
6	0.9974	0.07188	0.07188	0.9974	-5.514	83.2	83.2	-8.09
7	0.9965	0.08322	0.08322	0.9965	-6.41	82.09	82.09	-9.401
8	0.9955	0.09427	0.09427	0.9955	-7.296	81.01	81.01	-10.69
9	0.9945	0.105	0.105	0.9945	-8.17	79.93	79.93	-11.96
10	0.9933	0.1154	0.1154	0.9933	-9.034	78.88	78.88	-13.21
11	0.9921	0.1255	0.1255	0.9921	-9.886	77.84	77.84	-14.43
12	0.9908	0.1352	0.1352	0.9908	-10.72	76.82	76.82	-15.63
13	0.9895	0.1445	0.1445	0.9895	-11.55	75.82	75.82	-16.81
14	0.9881	0.1535	0.1535	0.9881	-12.35	74.85	74.85	-17.95
15	0.9868	0.1621	0.1621	0.9868	-13.15	73.89	73.89	-19.07
16	0.9854	0.1703	0.1703	0.9854	-13.93	72.95	72.95	-20.16
17	0.984	0.1782	0.1782	0.984	-14.7	72.04	72.04	-21.23
18	0.9826	0.1858	0.1858	0.9826	-15.45	71.14	71.14	-22.27
19	0.9812	0.1931	0.1931	0.9812	-16.19	70.26	70.26	-23.29
20	0.9798	0.2001	0.2001	0.9798	-16.92	69.39	69.39	-24.29
(Error percentage of the two results)(%)								
5	1.689e-06	1.653e-06	1.653e-06	1.103e-06	9.096e-05	8.396e-05	8.396e-05	8.295e-05
6	2.419e-06	6.909e-08	6.909e-08	1.885e-06	9.454e-05	8.607e-05	8.607e-05	9.046e-05
7	1.799e-06	1.721e-06	1.721e-06	1.439e-06	8.668e-05	8.28e-05	8.28e-05	8.326e-05
8	2.114e-06	2.34e-06	2.34e-06	4.224e-07	8.074e-05	8.589e-05	8.589e-05	8.765e-05
9	2.076e-06	3.124e-06	3.124e-06	1.423e-06	8.262e-05	8.614e-05	8.614e-05	8.828e-05
10	5.887e-07	5.068e-07	5.068e-07	2.417e-06	9.115e-05	8.753e-05	8.753e-05	8.938e-05
11	1.456e-06	2.557e-06	2.557e-06	2.187e-06	8.932e-05	8.517e-05	8.517e-05	7.91e-05
12	1.922e-06	4.003e-06	4.003e-06	2.035e-06	8.29e-05	8.139e-05	8.139e-05	9.041e-05
13	2.509e-07	8.91e-07	8.91e-07	1.626e-06	8.804e-05	8.752e-05	8.752e-05	8.076e-05
14	7.967e-07	9.406e-07	9.406e-07	3.096e-06	8.959e-05	8.509e-05	8.509e-05	8.904e-05
15	5.005e-07	1.332e-06	1.332e-06	2.326e-06	8.509e-05	8.379e-05	8.379e-05	8.179e-05
16	2.572e-07	1.224e-06	1.224e-06	1.632e-06	8.63e-05	8.826e-05	8.826e-05	8.379e-05
17	2.598e-06	2.008e-06	2.008e-06	1.598e-07	7.877e-05	8.448e-05	8.448e-05	8.584e-05
18	1.619e-06	2.125e-06	2.125e-06	3.804e-07	8.208e-05	9.083e-05	9.083e-05	8.687e-05
19	1.08e-06	9.936e-08	9.936e-08	3.301e-07	8.914e-05	9.191e-05	9.191e-05	8.77e-05
20	1.203e-06	4.483e-07	4.483e-07	7.221e-07	9.081e-05	9.044e-05	9.044e-05	8.667e-05

TABLE II

".geo" FILES GENERATED FOR AN ASYMMETRICAL MICROSTRIP GAP AT p_2 (OFF-GRID) FROM THE UDE AND LE APPROACH

LE: empl_11.geo.*n*					correspondence	UDE: agap_1.in.*n*				
n	W_1	W_2	S	H	(identical)	*n*	W_1	W_2	S	H
3	20	32	4	10	←----------→	0	20	32	4	10
0	16	32	4	10	←----------→	1	16	32	4	10
1	20	28	4	10	←----------→	2	20	28	4	10
2	20	32	6	10	←----------→	3	20	32	6	10

TABLE III

SIMULATION RESULTS FOR AN ASYMMETRICAL MICROSTRIP GAP AT p_2 (OFF-GRID) FROM THE UDE AND LE APPROACH

f (GHz)	$\|S_{11}\|$	$\|S_{12}\|$	$\|S_{21}\|$	$\|S_{22}\|$	θ_{11}	θ_{12}	θ_{21}	θ_{22}
(Results from the LE approach)								
5	0.9976	0.06843	0.06843	0.9976	-5.483	83.48	83.48	-7.554
6	0.9966	0.0815	0.0815	0.9966	-6.56	82.2	82.2	-9.034
7	0.9955	0.09426	0.09426	0.9955	-7.623	80.94	80.94	-10.49
8	0.9942	0.1067	0.1067	0.9942	-8.674	79.7	79.7	-11.93
9	0.9928	0.1187	0.1187	0.9928	-9.707	78.48	78.48	-13.33
10	0.9914	0.1303	0.1303	0.9914	-10.73	77.28	77.28	-14.72
11	0.9898	0.1414	0.1414	0.9898	-11.73	76.1	76.1	-16.07
12	0.9882	0.1521	0.1521	0.9882	-12.71	74.94	74.94	-17.39
13	0.9865	0.1623	0.1623	0.9865	-13.68	73.81	73.81	-18.69
14	0.9849	0.1721	0.1721	0.9849	-14.64	72.71	72.71	-19.95
15	0.9832	0.1814	0.1814	0.9832	-15.57	71.63	71.63	-21.18
16	0.9815	0.1903	0.1903	0.9815	-16.48	70.57	70.57	-22.38
17	0.9797	0.1988	0.1988	0.9797	-17.37	69.54	69.54	-23.55
18	0.978	0.2068	0.2068	0.978	-18.25	68.54	68.54	-24.66
19	0.9763	0.2146	0.2146	0.9763	-19.12	67.54	67.54	-25.8
20	0.9746	0.222	0.222	0.9746	-19.97	66.57	66.57	-26.9
(Results from the LE approach)								
5	0.9976	0.06843	0.06843	0.9976	-5.483	83.46	83.46	-7.554
6	0.9966	0.0815	0.0815	0.9966	-6.56	82.18	82.18	-9.033
7	0.9955	0.09426	0.09426	0.9955	-7.623	80.91	80.91	-10.49
8	0.9942	0.1067	0.1067	0.9942	-8.674	79.67	79.67	-11.93
9	0.9928	0.1187	0.1187	0.9928	-9.706	78.44	78.44	-13.33
10	0.9913	0.1303	0.1303	0.9913	-10.73	77.24	77.24	-14.72
11	0.9898	0.1414	0.1414	0.9898	-11.73	76.05	76.05	-16.07
12	0.9881	0.1521	0.1521	0.9881	-12.71	74.9	74.9	-17.39
13	0.9865	0.1623	0.1623	0.9865	-13.68	73.76	73.76	-18.69
14	0.9848	0.1721	0.1721	0.9848	-14.64	72.65	72.65	-19.95
15	0.9831	0.1814	0.1814	0.9831	-15.57	71.57	71.57	-21.18
16	0.9813	0.1903	0.1903	0.9814	-16.48	70.51	70.51	-22.38
17	0.9796	0.1987	0.1987	0.9796	-17.37	69.47	69.47	-23.55
18	0.9779	0.2068	0.2068	0.9779	-18.25	68.48	68.48	-24.66
19	0.9762	0.2146	0.2146	0.9762	-19.11	67.47	67.47	-25.8
20	0.9745	0.222	0.222	0.9745	-19.97	66.5	66.5	-26.89
(Error percentage of the two results)(%)								
5	0.001283	0.000721	0.000721	0.001222	0.001868	0.02477	0.02477	0.001161
6	0.001843	0.001048	0.001048	0.001773	0.00261	0.03011	0.03011	0.001587
7	0.002467	0.001397	0.001397	0.002382	0.003436	0.03555	0.03555	0.002106
8	0.003185	0.001797	0.001797	0.003092	0.004403	0.04091	0.04091	0.002685
9	0.003941	0.002216	0.002216	0.003765	0.005401	0.04629	0.04629	0.003256
10	0.0048	0.002688	0.002688	0.004611	0.006523	0.05194	0.05194	0.003941
11	0.005721	0.003181	0.003181	0.005453	0.007677	0.05758	0.05758	0.004662
12	0.006645	0.003687	0.003687	0.006303	0.008833	0.06318	0.06318	0.00534
13	0.007591	0.004202	0.004202	0.007206	0.01002	0.06887	0.06887	0.006087
14	0.008712	0.004743	0.004743	0.008165	0.01132	0.07468	0.07468	0.006861
15	0.009733	0.005285	0.005285	0.009191	0.01258	0.08043	0.08043	0.007643
16	0.01077	0.00585	0.00585	0.01012	0.01382	0.08626	0.08626	0.008415
17	0.01187	0.006412	0.006412	0.01104	0.01503	0.09218	0.09218	0.009116
18	0.01302	0.006932	0.006932	0.01191	0.01628	0.09827	0.09827	0.01002
19	0.01411	0.007529	0.007529	0.01299	0.01745	0.1042	0.1042	0.0107
20	0.01527	0.008111	0.008111	0.01414	0.01873	0.1103	0.1103	0.01153

TABLE IV

".geo" FILES GENERATED FOR AN ASYMMETRICAL MICROSTRIP GAP AT p_3 (OFF-GRID) FROM THE UDE AND LE APPROACH

LE: empl_11.geo.n					LE: nominal snapping point is represented by empl_11.geo.3. UDE: nominal snapping point is represented by agap_1.in.0	UDE: agap_1.in.n				
n	W_1	W_2	S	H		n	W_1	W_2	S	H
3	20	28	2	10		0	20	32	4	10
0	16	28	2	10		1	16	32	4	10
1	20	32	2	10		2	20	28	4	10
2	20	28	4	10		3	20	32	2	10

TABLE V

SIMULATION RESULTS FOR AN ASYMMETRICAL MICROSTRIP GAP AT p_3 (OFF-GRID) FROM THE UDE AND LE APPROACH

f (GHz)	$\lvert S_{11}\rvert$	$\lvert S_{12}\rvert$	$\lvert S_{21}\rvert$	$\lvert S_{22}\rvert$	θ_{11}	θ_{12}	θ_{21}	θ_{22}
(Results from the LE approach)								
5	0.9962	0.08415	0.08415	0.9962	-5.653	83.24	83.24	-7.875
6	0.9945	0.1003	0.1003	0.9945	-6.756	81.92	81.92	-9.4
7	0.9927	0.1161	0.1161	0.9927	-7.852	80.62	80.62	-10.92
8	0.9906	0.1315	0.1315	0.9906	-8.923	79.33	79.33	-12.41
9	0.9883	0.1465	0.1465	0.9883	-9.985	78.07	78.07	-13.87
10	0.9858	0.1611	0.1611	0.9858	-11.02	76.84	76.84	-15.3
11	0.9832	0.1751	0.1751	0.9832	-12.04	75.62	75.62	-16.7
12	0.9805	0.1887	0.1887	0.9805	-13.05	74.43	74.43	-18.08
13	0.9777	0.2017	0.2017	0.9777	-14.04	73.27	73.27	-19.43
14	0.9748	0.2142	0.2142	0.9748	-14.99	72.14	72.14	-20.73
15	0.9718	0.2263	0.2263	0.9718	-15.94	71.03	71.03	-22
16	0.9688	0.2378	0.2378	0.9688	-16.86	69.95	69.95	-23.24
17	0.9657	0.2489	0.2489	0.9657	-17.76	68.89	68.89	-24.44
18	0.9626	0.2596	0.2596	0.9626	-18.65	67.87	67.87	-25.6
19	0.9595	0.2699	0.2699	0.9595	-19.51	66.86	66.86	-26.77
20	0.9564	0.2798	0.2798	0.9564	-20.36	65.87	65.87	-27.89
(Error percentage of the two results)(%)								
5	0.9965	0.08179	0.08179	0.9964	-5.545	83.22	83.22	-7.774
6	0.9951	0.09751	0.09751	0.9949	-6.631	81.9	81.9	-9.295
7	0.9934	0.1129	0.1129	0.9931	-7.707	80.59	80.59	-10.8
8	0.9915	0.1279	0.1279	0.9911	-8.76	79.3	79.3	-12.27
9	0.9895	0.1425	0.1425	0.989	-9.804	78.03	78.03	-13.72
10	0.9873	0.1566	0.1566	0.9867	-10.82	76.79	76.79	-15.13
11	0.9849	0.1703	0.1703	0.9843	-11.83	75.57	75.57	-16.52
12	0.9825	0.1835	0.1835	0.9817	-12.82	74.38	74.38	-17.89
13	0.9799	0.1963	0.1963	0.979	-13.8	73.21	73.21	-19.21
14	0.9773	0.2085	0.2085	0.9763	-14.74	72.08	72.08	-20.51
15	0.9746	0.2203	0.2203	0.9735	-15.68	70.96	70.96	-21.77
16	0.9719	0.2315	0.2315	0.9707	-16.59	69.88	69.88	-23
17	0.9692	0.2424	0.2424	0.9678	-17.48	68.82	68.82	-24.19
18	0.9664	0.2528	0.2528	0.965	-18.36	67.79	67.79	-25.34
19	0.9636	0.2629	0.2629	0.962	-19.21	66.77	66.77	-26.5
20	0.9608	0.2727	0.2727	0.9591	-20.05	65.78	65.78	-27.6
(Error percentage of the two results)(%)								
5	0.03862	2.805	2.805	0.02288	1.896	0.01587	0.01587	1.278
6	0.05497	2.797	2.797	0.03264	1.855	0.03046	0.03046	1.12
7	0.07391	2.791	2.791	0.04383	1.846	0.03893	0.03893	1.093
8	0.09542	2.776	2.776	0.05663	1.828	0.04462	0.04462	1.099
9	0.1189	2.761	2.761	0.07085	1.815	0.04726	0.04726	1.108
10	0.1444	2.751	2.751	0.08666	1.823	0.05732	0.05732	1.089
11	0.1718	2.736	2.736	0.1031	1.749	0.06537	0.06537	1.078
12	0.2004	2.719	2.719	0.1208	1.734	0.07129	0.07129	1.1
13	0.2307	2.702	2.702	0.1395	1.72	0.07798	0.07798	1.097
14	0.262	2.685	2.685	0.1588	1.677	0.08606	0.08606	1.076
15	0.2939	2.666	2.666	0.1787	1.641	0.0952	0.0952	1.06
16	0.3271	2.648	2.648	0.2002	1.61	0.1039	0.1039	1.049
17	0.3612	2.628	2.628	0.2216	1.612	0.1131	0.1131	1.042
18	0.3949	2.606	2.606	0.2451	1.562	0.1177	0.1177	1.038
19	0.4299	2.583	2.583	0.2654	1.517	0.1321	0.1321	1.02
20	0.4646	2.557	2.557	0.2873	1.501	0.1453	0.1453	1.005

TABLE VI

SIMULATION RESULTS FOR A MITERED MICROSTRIP BEND AT p_4 FROM THE UDE AND LE APPROACH

f (GHz)	$\lvert S_{11}\rvert$	$\lvert S_{12}\rvert$	$\lvert S_{21}\rvert$	$\lvert S_{22}\rvert$	θ_{11}	θ_{12}	θ_{21}	θ_{22}
(Results from the LE approach)								
5	0.3141	0.9494	0.9494	0.3141	-120.5	-30.42	-30.42	-120.5
6	0.3655	0.9308	0.9308	0.3655	-126.1	-36.08	-36.08	-126.1
7	0.4119	0.9112	0.9112	0.4119	-131.6	-41.55	-41.55	-131.6
8	0.4533	0.8913	0.8913	0.4533	-136.8	-46.83	-46.83	-136.8
9	0.4898	0.8718	0.8718	0.4898	-141.9	-51.93	-51.93	-141.9
10	0.5216	0.8532	0.8532	0.5216	-146.9	-56.87	-56.87	-146.9
11	0.5488	0.8359	0.8359	0.5488	-151.7	-61.65	-61.65	-151.7
12	0.5718	0.8204	0.8204	0.5718	-156.3	-66.31	-66.31	-156.3
13	0.5908	0.8068	0.8068	0.5908	-160.9	-70.85	-70.85	-160.9
14	0.606	0.7955	0.7955	0.606	-165.3	-75.32	-75.32	-165.3
15	0.6175	0.7866	0.7866	0.6175	-169.7	-79.74	-79.74	-169.7
16	0.6254	0.7803	0.7803	0.6254	-174.1	-84.14	-84.14	-174.1
17	0.6298	0.7768	0.7768	0.6298	-178.5	-88.54	-88.54	-178.5
18	0.6305	0.7762	0.7762	0.6305	177	-92.98	-92.98	177
19	0.6275	0.7787	0.7787	0.6275	172.5	-97.49	-97.49	172.5
20	0.6203	0.7843	0.7843	0.6203	167.9	-102.1	-102.1	167.9
(Results from the LE approach)								
5	0.3141	0.9494	0.9494	0.3141	-120.4	-30.43	-30.43	-120.4
6	0.3655	0.9308	0.9308	0.3655	-126.1	-36.08	-36.08	-126.1
7	0.4119	0.9112	0.9112	0.4119	-131.5	-41.55	-41.55	-131.6
8	0.4533	0.8913	0.8913	0.4533	-136.8	-46.83	-46.83	-136.8
9	0.4898	0.8718	0.8718	0.4898	-141.9	-51.93	-51.93	-141.9
10	0.5216	0.8532	0.8532	0.5216	-146.9	-56.87	-56.87	-146.9
11	0.5489	0.8359	0.8359	0.5489	-151.7	-61.65	-61.65	-151.7
12	0.5718	0.8204	0.8204	0.5718	-156.3	-66.31	-66.31	-156.3
13	0.5908	0.8068	0.8068	0.5908	-160.9	-70.86	-70.86	-160.9
14	0.606	0.7955	0.7955	0.606	-165.3	-75.33	-75.33	-165.3
15	0.6175	0.7866	0.7866	0.6175	-169.7	-79.74	-79.74	-169.7
16	0.6254	0.7803	0.7803	0.6254	-174.1	-84.14	-84.14	-174.1
17	0.6298	0.7768	0.7768	0.6298	-178.5	-88.54	-88.54	-178.5
18	0.6305	0.7762	0.7762	0.6305	177	-92.98	-92.98	177
19	0.6275	0.7786	0.7786	0.6275	172.5	-97.5	-97.5	172.5
20	0.6203	0.7843	0.7843	0.6203	167.9	-102.1	-102.1	167.9
(Error percentage of the two results)(%)								
5	0.001556	0.0002762	0.0002762	0.001556	0.04989	0.02293	0.02293	0.04989
6	0.004682	0.0005165	0.0005165	0.004682	0.007844	0.005611	0.005611	0.007844
7	0.002044	0.0001441	0.0001441	0.002043	0.04569	0.002502	0.002502	0.03032
8	0.001085	9.535e-05	9.535e-05	0.001085	0.007235	0.006331	0.006331	0.007235
9	0.0005486	0.0004255	0.0004255	0.0005486	0.006958	0.00586	0.00586	0.006958
10	0.0007647	0.0005806	0.0005806	0.0007647	0.006721	0.006947	0.006947	0.006721
11	0.002902	0.0008252	0.0008252	0.002902	0.006503	0.001544	0.001544	0.006503
12	0.001366	0.0002131	0.0002131	0.001366	0.006316	0.001423	0.001423	0.006316
13	0.0004252	0.0002044	0.0002044	0.0004252	0.006128	0.01121	0.01121	0.006128
14	0.001876	0.0007321	0.0007321	0.001876	0.01217	0.006561	0.006561	0.01217
15	0.002824	0.002131	0.002131	0.002824	0.01187	0.006349	0.006349	0.01187
16	0.001689	0.0007653	0.0007653	0.001689	0.01157	0.002288	0.002288	0.01157
17	0.001585	0.000712	0.000712	0.001585	0.01128	0.001213	0.001213	0.01128
18	0.001437	0.001116	0.001116	0.001434	0.002175	0.003149	0.003149	0.00217
19	0.0005099	0.0002753	0.0002753	0.0005163	8.359e-05	0.007093	0.007093	9.729e-05
20	0.0007572	0.000486	0.000486	0.0007568	0.003476	0.01968	0.01968	0.002467

TABLE VII

SIMULATION ERROR FOR AN MICROSTRIP DOUBLE PATCH CAPACITOR AT POINT p_5 BETWEEN THE UDE AND LE APPROACH

f (GHz)	$\lvert S_{11}\rvert$	$\lvert S_{12}\rvert$	$\lvert S_{21}\rvert$	$\lvert S_{22}\rvert$	θ_{11}	θ_{12}	θ_{21}	θ_{22}
(Error percentage of the two results)(%)								
0.5	6.776e-08	2.214e-06	2.214e-06	1.97e-06	8.389e-05	8.803e-05	8.803e-05	9.058e-05
1.5	2.781e-06	1.112e-06	1.112e-06	8.131e-08	8.514e-05	8.896e-05	8.896e-05	8.326e-05
2.5	1.512e-06	1.716e-06	1.716e-06	1.049e-06	9.025e-05	8.408e-05	8.408e-05	8.859e-05
3.5	1.174e-06	1.815e-06	1.815e-06	2.136e-07	8.687e-05	8.776e-05	8.776e-05	8.488e-05
4.5	2.954e-06	1.176e-07	1.176e-07	9.814e-07	8.614e-05	8.73e-05	8.73e-05	8.438e-05
5.5	2.435e-06	2.636e-06	2.636e-06	1.917e-07	8.31e-05	8.101e-05	8.101e-05	8.897e-05
6.5	8.21e-08	2.497e-06	2.497e-06	2.42e-06	8.428e-05	8.634e-05	8.634e-05	8.784e-05
7.5	2.85e-06	8.421e-07	8.421e-07	7.087e-07	8.754e-05	8.559e-05	8.559e-05	9.09e-05
8.5	8.183e-07	4.836e-06	4.836e-06	4.001e-06	8.414e-05	8.923e-05	8.923e-05	8.878e-05
9.5	1.169e-06	8.976e-08	8.976e-08	2.558e-06	8.275e-05	9.2e-05	9.2e-05	8.523e-05
10.5	1.784e-06	2.548e-06	2.548e-06	1.759e-06	8.519e-05	8.413e-05	8.413e-05	8.653e-05
11.5	5.759e-07	2.333e-06	2.333e-06	9.717e-07	8.75e-05	8.531e-05	8.531e-05	8.213e-05
12.5	3.045e-07	2.142e-06	2.142e-06	9.015e-07	8.955e-05	8.497e-05	8.497e-05	8.439e-05
13.5	2.769e-06	7.55e-07	7.55e-07	6.758e-07	8.891e-05	8.487e-05	8.487e-05	8.664e-05
14.5	1.422e-07	8.787e-07	8.787e-07	5.116e-07	8.655e-05	8.703e-05	8.703e-05	8.33e-05
15.5	1.93e-06	1.222e-07	1.222e-07	1.393e-06	8.725e-05	8.986e-05	8.986e-05	8.353e-05
16.5	1.535e-06	2.454e-06	2.454e-06	1.052e-06	8.239e-05	9.35e-05	9.35e-05	8.801e-05
17.5	1.207e-06	2.216e-06	2.216e-06	2.576e-07	8.298e-05	8.288e-05	8.288e-05	8.741e-05
18.5	2.061e-06	2.928e-06	2.928e-06	5.393e-07	8.555e-05	8.79e-05	8.79e-05	8.888e-05
19.5	2.577e-07	2.045e-06	2.045e-06	2.476e-07	8.979e-05	8.631e-05	8.631e-05	8.405e-05
20.5	7.022e-08	2.303e-06	2.303e-06	1.981e-06	8.683e-05	8.635e-05	8.635e-05	8.817e-05
21.5	1.147e-06	3.99e-06	3.99e-06	1.664e-06	8.806e-05	8.308e-05	8.308e-05	8.747e-05
22.5	4.598e-07	2.025e-06	2.025e-06	8.662e-07	8.809e-05	8.462e-05	8.462e-05	8.651e-05
23.5	1.329e-07	3.716e-06	3.716e-06	1.506e-06	8.964e-05	8.974e-05	8.974e-05	8.337e-05
24.5	2.874e-06	1.103e-06	1.103e-06	2.667e-07	8.48e-05	8.755e-05	8.755e-05	8.528e-05
25.5	1.852e-06	2.924e-06	2.924e-06	2.843e-06	8.928e-05	8.502e-05	8.502e-05	8.246e-05
26.5	2.576e-06	6.48e-07	6.48e-07	2.795e-06	8.426e-05	8.919e-05	8.919e-05	8.472e-05
27.5	2.543e-06	1.571e-06	1.571e-06	5.202e-07	8.36e-05	8.427e-05	8.427e-05	8.971e-05
28.5	1.794e-07	2.834e-06	2.834e-06	8.229e-08	8.488e-05	8.851e-05	8.851e-05	8.457e-05
29.5	7.86e-07	1.116e-06	1.116e-06	1.659e-06	8.633e-05	8.31e-05	8.31e-05	8.852e-05
30.5	1.898e-06	2.801e-06	2.801e-06	2.214e-06	8.46e-05	8.389e-05	8.389e-05	8.873e-05
31.5	3.534e-07	6.699e-07	6.699e-07	2.776e-06	8.717e-05	8.778e-05	8.778e-05	8.424e-05
32.5	4.954e-07	4.031e-06	4.031e-06	2.444e-06	8.495e-05	8.477e-05	8.477e-05	8.939e-05
33.5	1.775e-06	4.861e-06	4.861e-06	1.816e-06	8.967e-05	8.369e-05	8.369e-05	8.168e-05
34.5	4.249e-07	4.429e-06	4.429e-06	2.28e-06	8.235e-05	8.738e-05	8.738e-05	8.83e-05
35.5	9.648e-07	1.591e-06	1.591e-06	2.384e-06	8.76e-05	8.131e-05	8.131e-05	8.997e-05
36.5	9.422e-07	6.431e-07	6.431e-07	1.151e-06	8.567e-05	8.952e-05	8.952e-05	8.859e-05
37.5	1.003e-06	1.646e-06	1.646e-06	2.158e-06	8.386e-05	8.643e-05	8.643e-05	8.638e-05
38.5	1.346e-06	1.058e-06	1.058e-06	1.414e-06	8.672e-05	8.223e-05	8.223e-05	8.175e-05
39.5	8.127e-07	9.672e-07	9.672e-07	1.186e-06	8.539e-05	8.742e-05	8.742e-05	8.47e-05
40.5	1.874e-06	9.642e-07	9.642e-07	5.587e-07	8.959e-05	8.8e-05	8.8e-05	8.631e-05
41.5	6.153e-07	1.759e-06	1.759e-06	2.346e-06	8.456e-05	8.482e-05	8.482e-05	8.767e-05
42.5	1.87e-06	2.562e-06	2.562e-06	9.632e-07	8.974e-05	8.411e-05	8.411e-05	8.045e-05
43.5	1.485e-06	2.77e-06	2.77e-06	1.774e-06	9.035e-05	8.085e-05	8.085e-05	8.49e-05
44.5	4.977e-07	1.512e-07	1.512e-07	1.303e-06	8.385e-05	8.748e-05	8.748e-05	8.548e-05
45.5	1.301e-06	1.112e-06	1.112e-06	1.488e-06	8.335e-05	8.719e-05	8.719e-05	8.768e-05
46.5	2.201e-06	2.048e-06	2.048e-06	1.915e-08	8.224e-05	8.447e-05	8.447e-05	8.909e-05
47.5	1.248e-06	1.215e-06	1.215e-06	2.788e-06	8.619e-05	8.963e-05	8.963e-05	8.52e-05
48.5	7.778e-07	2.103e-06	2.103e-06	2.877e-06	8.535e-05	8.673e-05	8.673e-05	8.593e-05
49.5	1.825e-06	2.434e-06	2.434e-06	1.769e-06	8.846e-05	8.591e-05	8.591e-05	9.065e-05

TABLE VIII

SIMULATION ERROR FOR A MICROSTRIP RECTANGULAR STRUCTURE AT p_8 BETWEEN THE UDE AND LE APPROACH

f (GHz)	$\lvert S_{11}\rvert$	$\lvert S_{12}\rvert$	$\lvert S_{21}\rvert$	$\lvert S_{22}\rvert$	θ_{11}	θ_{12}	θ_{21}	θ_{22}
(Error percentage of the two results)(%)								
0.5	3.921e-06	2.935e-06	2.935e-06	3.968e-06	8.924e-05	8.508e-05	8.508e-05	8.988e-05
2.5	1.992e-06	9.156e-07	9.156e-07	1.389e-06	8.531e-05	8.764e-05	8.764e-05	8.268e-05
4.5	2.304e-06	2.3e-07	2.3e-07	3.202e-06	8.286e-05	8.123e-05	8.123e-05	8.731e-05
6.5	2.071e-06	1.939e-07	1.939e-07	3.345e-07	9.025e-05	9.353e-05	9.353e-05	8.709e-05
8.5	2.702e-06	4.855e-06	4.855e-06	6.124e-07	8.714e-05	8.129e-05	8.129e-05	8.891e-05
10.5	1.866e-07	4.425e-06	4.425e-06	3.365e-06	8.794e-05	8.642e-05	8.642e-05	8.867e-05
12.5	2.624e-06	1.047e-06	1.047e-06	4.903e-07	8.67e-05	8.395e-05	8.395e-05	8.894e-05
14.5	2.145e-06	5.622e-07	5.622e-07	3.049e-06	8.695e-05	8.844e-05	8.844e-05	8.962e-05
16.5	3.097e-07	5.699e-07	5.699e-07	5.583e-07	8.423e-05	8.91e-05	8.91e-05	8.334e-05
18.5	1.722e-06	2.508e-06	2.508e-06	4.572e-07	8.903e-05	8.404e-05	8.404e-05	8.228e-05
20.5	2.497e-06	2.304e-06	2.304e-06	2.238e-06	8.448e-05	8.686e-05	8.686e-05	8.891e-05
22.5	1.209e-06	1.814e-07	1.814e-07	8.575e-07	8.253e-05	8.435e-05	8.435e-05	8.919e-05
24.5	3.28e-06	3.875e-07	3.875e-07	8.005e-07	8.84e-05	8.547e-05	8.547e-05	9.056e-05
26.5	2.669e-06	3.795e-06	3.795e-06	1.532e-06	8.031e-05	8.419e-05	8.419e-05	8.233e-05
28.5	1.183e-06	3.084e-06	3.084e-06	1.393e-06	8.431e-05	8.613e-05	8.613e-05	8.381e-05
30.5	3.911e-06	2.573e-07	2.573e-07	2.88e-06	8.336e-05	8.268e-05	8.268e-05	8.218e-05
32.5	3.077e-06	2.979e-06	2.979e-06	1.075e-06	8.084e-05	8.746e-05	8.746e-05	9.102e-05
34.5	2.235e-07	4.307e-06	4.307e-06	1.386e-06	9.064e-05	8.859e-05	8.859e-05	8.484e-05
36.5	7.95e-07	1.606e-07	1.606e-07	2.482e-06	8.906e-05	8.405e-05	8.405e-05	8.595e-05
38.5	1.054e-06	1.76e-07	1.76e-07	3.336e-06	8.378e-05	8.436e-05	8.436e-05	8.571e-05
40.5	4.654e-07	2.675e-06	2.675e-06	3.031e-06	8.981e-05	8.377e-05	8.377e-05	8.595e-05
42.5	2.773e-06	4.688e-07	4.688e-07	3.569e-06	8.479e-05	8.403e-05	8.403e-05	8.583e-05
44.5	2.84e-06	4.238e-06	4.238e-06	1.851e-06	8.571e-05	8.75e-05	8.75e-05	8.175e-05
46.5	1.197e-06	2.647e-06	2.647e-06	2.833e-07	8.734e-05	8.186e-05	8.186e-05	7.947e-05
48.5	7.23e-07	4.067e-06	4.067e-06	2.734e-06	8.929e-05	8.951e-05	8.951e-05	8.363e-05
50.5	1.038e-06	3.414e-06	3.414e-06	2.617e-06	8.991e-05	8.541e-05	8.541e-05	8.25e-05

TABLE IX

SIMULATION ERROR FOR A MICROSTRIP INTERDIGITAL CAPACITOR AT p_9 BETWEEN THE UDE AND LE APPROACH

f (GHz)	$\lvert S_{11}\rvert$	$\lvert S_{12}\rvert$	$\lvert S_{21}\rvert$	$\lvert S_{22}\rvert$	θ_{11}	θ_{12}	θ_{21}	θ_{22}
(Error percentage of the two results)(%)								
0.5	1.093e-06	0.03209	0.03209	3.936e-07	0.1729	0.06903	0.06903	0.1016
2.5	0.0002019	0.0287	0.0287	0.0002035	8.188e-05	8.376e-05	8.376e-05	8.639e-05
4.5	0.0001998	0.04104	0.04104	0.0002011	8.707e-05	0.01853	0.01853	8.93e-05
6.5	0.0002963	0.08259	0.08259	0.0002991	8.742e-05	8.854e-05	8.854e-05	8.183e-05
8.5	0.0009	0.1528	0.1528	0.0006048	8.244e-05	0.01219	0.01219	8.336e-05
10.5	0.002105	0.2823	0.2823	0.00211	0.00563	0.01085	0.01085	0.005497
12.5	0.01333	0.6712	0.6712	0.004853	0.01217	8.775e-05	8.775e-05	0.02997
14.5	1.961	6.608	6.608	1.964	0.6908	1.498	1.498	2.762
16.5	8.993	0.1142	0.1142	8.925	3.539	0.4269	0.4269	7.824
18.5	0.304	0.2141	0.2141	0.2905	0.373	0.2257	0.2257	0.1187
20.5	0.3239	0.4247	0.4247	0.322	0.09624	0.4384	0.4384	0.1343
22.5	0.009811	0.1293	0.1293	0.005523	0.06111	8.402e-05	8.402e-05	0.05681
24.5	0.0008056	0.1091	0.1091	0.0007023	0.01126	8.557e-05	8.557e-05	0.01154
26.5	0.0008035	0.01139	0.01139	0.001703	0.02387	8.771e-05	8.771e-05	0.006036
28.5	0.001004	0.05774	0.05774	0.001103	0.02532	8.413e-05	8.413e-05	0.01282
30.5	0.002202	0.08694	0.08694	0.0005023	0.02706	8.619e-05	8.619e-05	0.02047
32.5	0.0001969	0.07649	0.07649	0.0001997	0.05182	9.009e-05	9.009e-05	0.03702
34.5	0.01797	0.06263	0.06263	0.0007088	0.1136	0.06492	0.06492	0.07576
36.5	0.002784	0.9267	0.9267	0.005157	0.2197	0.08738	0.08738	0.2587
38.5	1.123	0.8001	0.8001	1.414	3.614	1.046	1.046	1.34
40.5	0.4934	0.2768	0.2768	0.1828	2.642	0.6896	0.6896	2.373
42.5	0.1948	1.461	1.461	0.3194	0.8168	11.44	11.44	1.494
44.5	0.5435	4.654	4.654	0.06581	0.3668	0.7709	0.7709	0.09173
46.5	0.8323	1.834	1.834	0.03182	3.529	2.199	2.199	8.376e-05
48.5	0.712	5.481	5.481	0.09864	3.639	4.432	4.432	8.212e-05
50.5	0.3509	28.23	28.23	0.05672	1.133	4.696	4.696	0.03612

TABLE X

SIMULATION ERROR FOR A MICROSTRIP OVERLAY DOUBLE PATCH CAPACITOR AT p_{10} BETWEEN THE UDE AND LE APPROACH

f (GHz)	$\lvert S_{11} \rvert$	$\lvert S_{12} \rvert$	$\lvert S_{21} \rvert$	$\lvert S_{22} \rvert$	θ_{11}	θ_{12}	θ_{21}	θ_{22}
(Error percentage of the two results)(%)								
0.5	0.0001002	0.03717	0.03717	0.0001041	0.06927	0.01976	0.01976	0.3478
2.5	0.001016	0.03149	0.03149	0.001017	0.1399	0.007878	0.007878	0.14
4.5	0.001119	0.02693	0.02693	0.001117	0.1127	0.03996	0.03996	0.1027
6.5	0.00102	0.02706	0.02706	0.001021	0.08423	8.197e-05	8.197e-05	0.0844
8.5	0.0008096	0.02813	0.02813	0.0008094	0.07527	8.786e-05	8.786e-05	8.88e-05
10.5	0.0006095	0.02897	0.02897	0.0006091	8.978e-05	0.01884	0.01884	0.07006
12.5	0.0005072	0.02839	0.02839	0.0005071	0.06636	8.307e-05	8.307e-05	0.06654
14.5	0.0004015	0.03105	0.03105	0.0004037	8.498e-05	8.364e-05	8.364e-05	0.06395
16.5	0.0003065	0.02886	0.02886	0.0003043	0.06179	0.01389	0.01389	0.06197
18.5	0.0003024	0.02953	0.02953	0.0003004	9.034e-05	8.931e-05	8.931e-05	0.06036
20.5	0.0002989	0.02965	0.02965	0.0003018	8.824e-05	8.772e-05	8.772e-05	0.05901
22.5	0.0003065	0.03024	0.03024	0.0003062	8.376e-05	8.267e-05	8.267e-05	0.05786
24.5	0.0003048	0.0303	0.0303	0.0003068	8.917e-05	0.01151	0.01151	0.05681
26.5	0.0003038	0.02982	0.02982	0.0003074	8.965e-05	8.733e-05	8.733e-05	0.05586
28.5	0.0004002	0.03648	0.03648	0.0003989	0.02821	8.835e-05	8.835e-05	0.02803
30.5	0.0004022	0.04	0.04	0.000402	0.03438	0.01044	0.01044	0.02278
32.5	0.0006067	0.04554	0.04554	0.0006055	0.03498	8.568e-05	8.568e-05	0.02899
34.5	0.0009075	0.04894	0.04894	0.0009091	0.04153	8.409e-05	8.409e-05	0.02952
36.5	0.001417	0.05748	0.05748	0.001414	0.04238	8.892e-05	8.892e-05	0.03012
38.5	0.001623	0.06681	0.06681	0.002233	0.04956	8.648e-05	8.648e-05	0.03701
40.5	0.00113	0.01926	0.01926	0.01166	0.06368	8.652e-05	8.652e-05	0.05079
42.5	0.007152	0.1036	0.1036	0.00746	0.09247	8.294e-05	8.294e-05	0.03951
44.5	0.01698	0.1225	0.1225	0.01665	0.1464	9.154e-05	9.154e-05	0.04171
46.5	0.03264	0.09569	0.09569	0.03311	0.4365	0.1434	0.1434	0.04585
48.5	0.5778	0.3281	0.3281	0.5788	0.02845	8.749e-05	8.749e-05	0.04764
50.5	0.3682	0.0624	0.0624	1.393	0.5679	0.08125	0.08125	0.6247

TABLE XI

LOSS PARAMETERS DEFINITION IN THE LE APPROACH AND UDE APPROACH

	Dielectric Loss Parameters	Metallization Loss Parameters
LE Approach	(1) Dielectric Loss Tangent: $\tan\delta$ $\tan\delta = \frac{\sigma_d}{\omega\varepsilon}$	(1) Conducting Metal Resistivity: ρ_c (Ω/m^3) $\rho_c = \frac{1}{\sigma_c}$
	(2) Magnetic Loss Tangent: Normally set to 0	(2) Surface Reactance: X_S (Ω/m^2) $X_S = \frac{1}{\sigma_c \delta_c}$
UDE Approach	(1) Dielectric Loss Tangent: $\tan\delta$	(1) DC: Metal Strip Unit Square Impedance: $R_{DC} + jX_{DC}$ (Ω/m^2) $R_{DC} = \frac{1}{\sigma_c t}$ $X_{DC} = 0$
		(2) AC: Metal Strip Unit Square Resistance (Skin Effect Impedance): R_S (Ω/m^2) $R_S = \frac{1}{\sigma_c \delta_c} = \sqrt{\pi \frac{f\mu}{\sigma_c}} = \sqrt{f}\, R_{RF}$ $R_{RF} = \sqrt{\pi \frac{\mu}{\sigma_c}}$ To be independent of frequency, R_{RF} is actually used to represent the AC Resistance.
Relation Between UDE and LE Loss Parameter		$R_{DC} = \begin{cases} 0 & t = 0 \\ \frac{\rho_c}{t} & t > 0 \end{cases}$ $R_{RF} = \sqrt{\pi \mu \rho_c}$

In the expression above:

ε —— dielectric constant.
μ —— conductor permeability.
σ_d —— dielectric (bulk) conductivity.
ω —— angular frequency.
σ_c —— conductor (bulk) conductivity.
t —— conductor thickness.
δ_c —— conductor skin depth ($\delta_c = \sqrt{\frac{2}{\mu\omega\sigma_c}}$).

TABLE XII

SIMULATION RESULTS FOR A LOSSY MICROSTRIP OPEN STUB AT p_{11} FROM THE UDE AND LE APPROACH

f (GHz)	$\lvert S_{11} \rvert$	θ_{11}	$\lvert S_{11} \rvert$	θ_{11}	$E_{\lvert S11 \rvert}$	$E_{\theta 11}$
	(Results from the UDE approach)		(Results from the LE approach)		(Error percentage of the two results)(%)	
0.5	0.9999	-7.655	0.9999	-7.655	3.68e-08	8.337e-05
2.5	0.9994	-37.53	0.9994	-37.53	1.137e-06	8.707e-05
4.5	0.9988	-65	0.9988	-65	2.443e-06	8.224e-05
6.5	0.9984	-89.25	0.9984	-89.25	1.652e-06	8.424e-05
8.5	0.9979	-110.3	0.9979	-110.3	3.331e-07	8.814e-05
10.5	0.9976	-128.7	0.9976	-128.7	0.0002014	8.506e-05
2.5	0.9972	-145.2	0.9972	-145.2	0.0002041	8.153e-05
4.5	0.9969	-160.3	0.9969	-160.3	0.0001043	8.383e-05
16.5	0.9965	-174.8	0.9965	-174.8	9.853e-07	8.529e-05
18.5	0.996	170.9	0.996	170.9	2.307e-06	8.541e-05
20.5	0.9954	156	0.9954	156	2.04e-06	8.923e-05
22.5	0.9946	139.8	0.9946	139.8	9.718e-05	8.209e-05
24.5	0.9935	121.6	0.9935	121.6	9.835e-05	8.823e-05
26.5	0.9921	100.3	0.9921	100.3	0.0002009	8.374e-05
28.5	0.9904	75.01	0.9904	75.01	0.0003018	8.383e-05
30.5	0.9888	45.46	0.9888	45.46	0.0004025	0.002111
32.5	0.9878	12.7	0.9879	12.7	0.0007129	0.01584
34.5	0.9879	-20.63	0.9879	-20.63	0.003343	8.482e-05
36.5	0.9888	-51.65	0.9888	-51.65	0.001313	9.109e-05
38.5	0.9899	-78.88	0.99	-78.88	0.001313	8.657e-05
40.5	0.991	-102.4	0.991	-102.4	9.935e-05	8.935e-05
42.5	0.9917	-123	0.9917	-123	0.0005066	8.952e-05
44.5	0.9921	-141.7	0.9921	-141.7	5.054e-08	9.127e-05
46.5	0.9923	-159.2	0.9923	-159.2	1.235e-06	8.274e-05
48.5	0.9922	-176.4	0.9922	-176.4	2.021e-06	8.752e-05
50.5	0.9701	166	0.9701	166	3.292e-07	8.889e-05

TABLE XIII

COMPARISON OF UDE AND LE APPROACH FOR A FILTER DESIGN

		UDE		LE
Number of polygons:		1		2
Maximum snapping points:		7		9
Modelling grid size:		1 × CELL:W L_1 S_1 S_2 2 × CELL:L_2 L_3		1 × CELL:W_1 W_2 W_3 L_1 L_2 L_3 S_1 S_2
Analysis time (user time) per frequency:		18 sec		19 sec
Number of frequencies:		26		26
Simulation at p_s:				
Snapping points:		4		6
Simulation real time under same CPU use percentage:		3 hours		5 hours
Optimization:				
Starting point:	p_s	L_1 = 84 mil L_2 = 80 mil L_3 = 80 mil S_1 = 4.8 mil S_2 = 4.8 mil	p_s	L_1 = 84 mil L_2 = 80 mil L_3 = 80 mil S_1 = 4.8 mil S_2 = 4.8 mil
Optimizer:		minimax		minimax
Perturbation scale:		1.0×10^{-4}		1.0×10^{-4}
Accuracy of solution:		0.0001		0.0001
Number of iterations:		10		10
Optimization real time under same CPU use percentage:		5 days		1 day
optimal point:		L_1 = 88.29 mil L_2 = 83.00 mil L_3 = 83.00 mil S_1 = 4.86 mil S_2 = 4.87 mil		L_1 = 88.81 mil L_2 = 81.90 mil L_3 = 81.90 mil S_1 = 4.86 mil S_2 = 4.86 mil

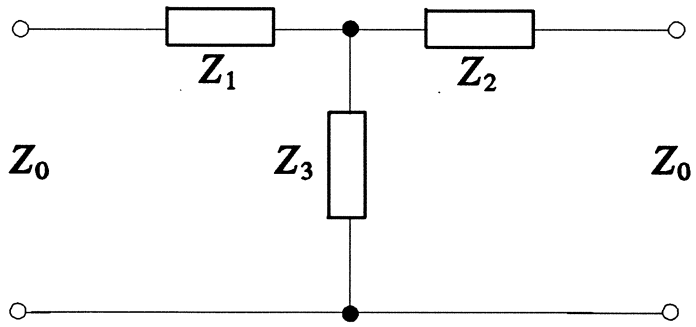

Fig. 1 (a) T-type equivalent network for microstrip elements.

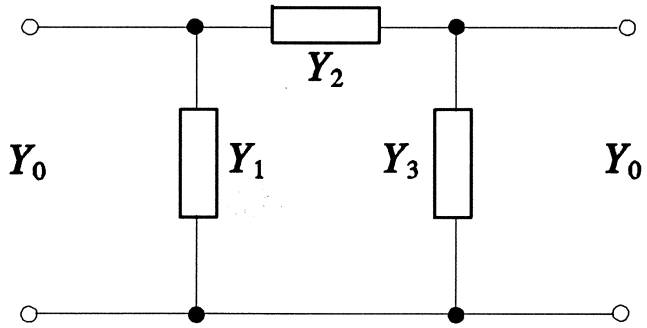

Fig. 1 (b) Π-type equivalent network for microstrip elements.

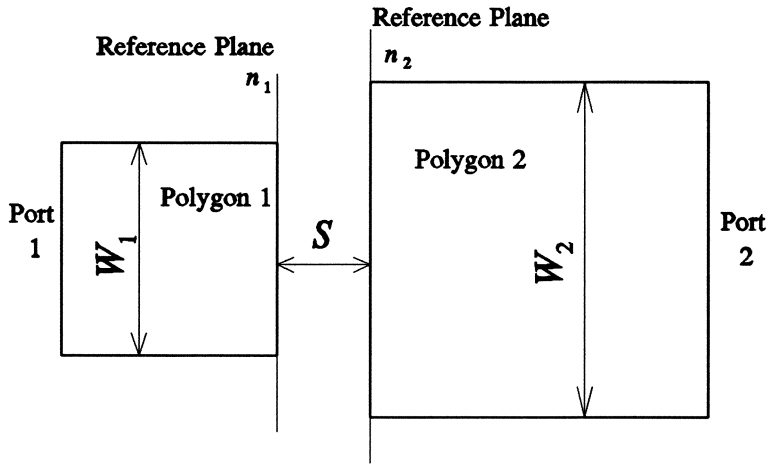

Fig. 2 (a) Structure of microstrip asymmetrical gap.

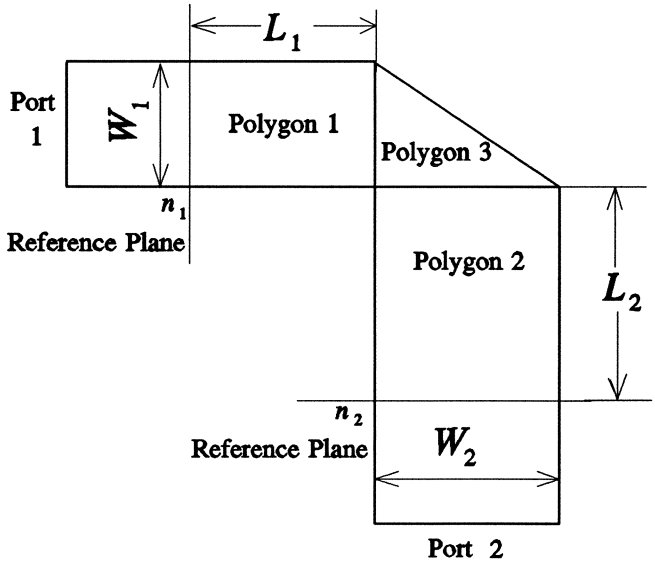

Fig. 2 (b) The structure of mitered microstrip bend.

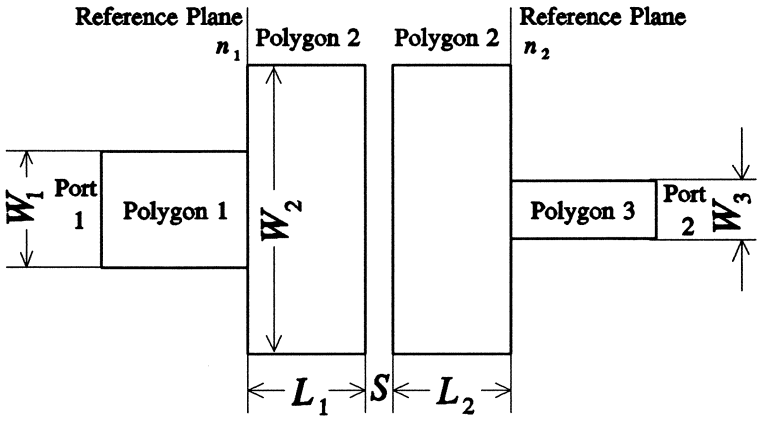

Fig. 2 (c) The structure of microstrip double patch capacitor.

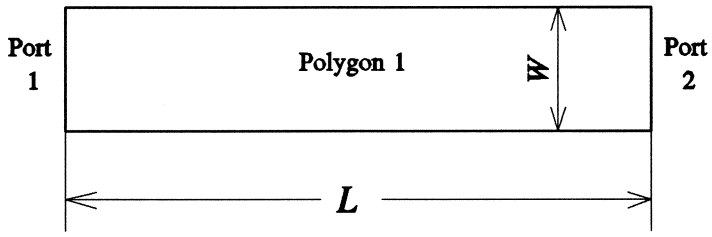

Fig. 2 (d) The structure of microstrip line.

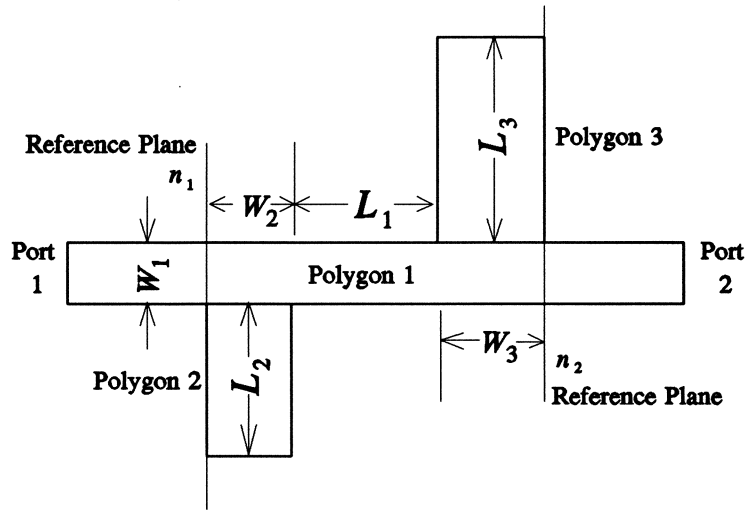

Fig. 2 (e) The structure of asymmetrical microstrip double stub.

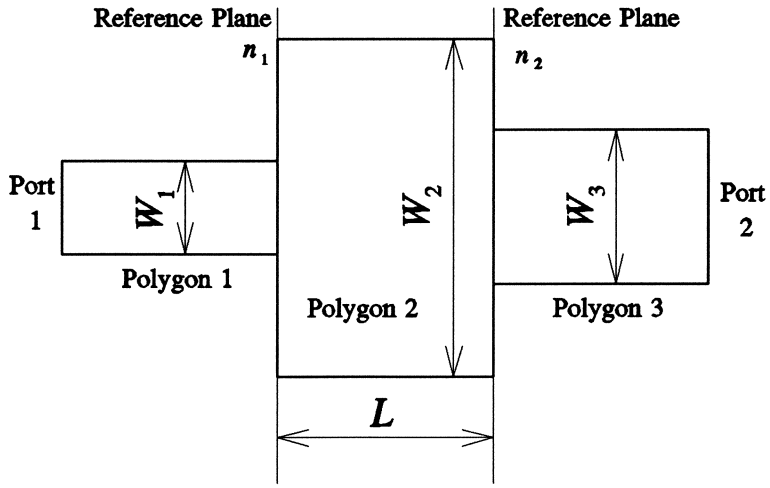

Fig. 2 (f) The structure of microstrip rectangular structure.

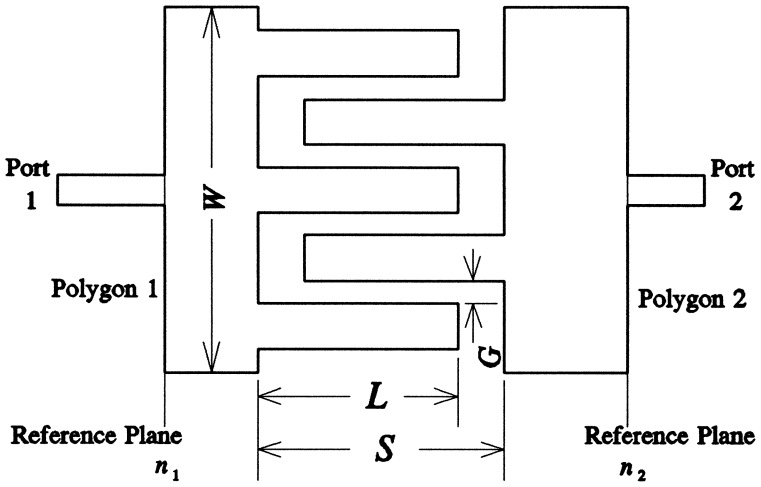

Fig. 2 (g) The structure of microstrip interdigital capacitor.

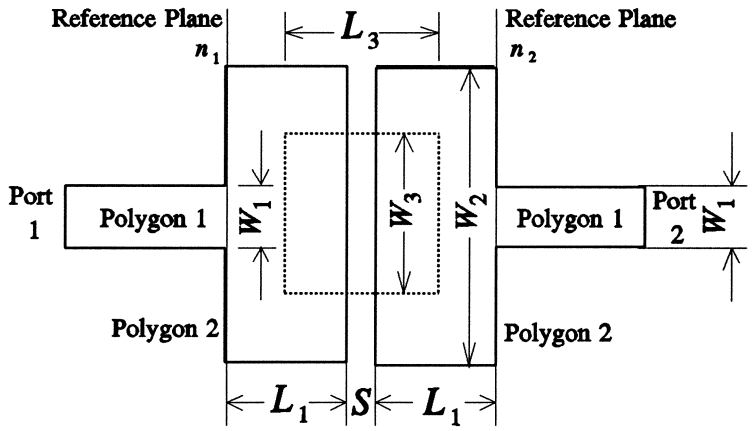

Fig. 2 (h) The structure of microstrip overlay double patch capacitor.

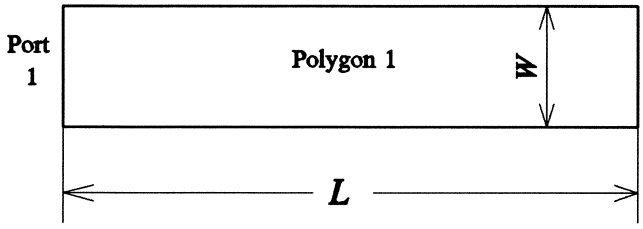

Fig. 2 (i) The structure of microstrip open stub.

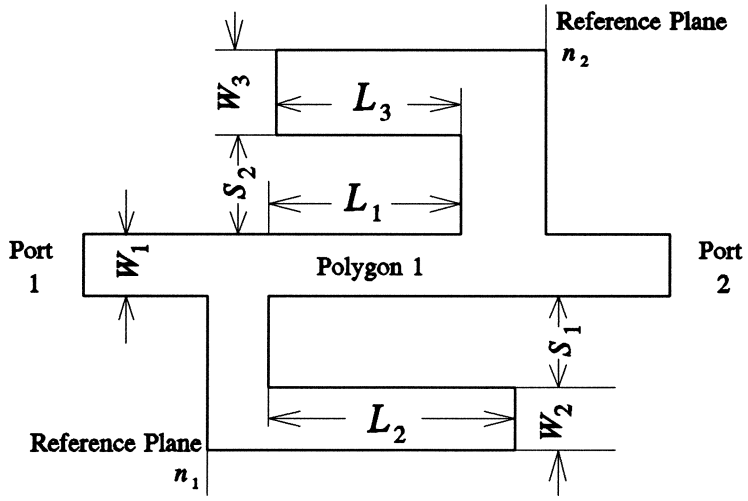

Fig. 2 (j) The structure of asymmetrical microstrip double stub.

```
VER 2.4a
LIC osa1.101
DAT Mon Jan 16 10:48:51 1995
LEN mil 2.5400000000e-05
SYM
REF 58.000000 58.000000 0.0000000 0.0000000 0.0000000 0.0000000 0.0000000 0.0000000
TOP 377 0 0
TON 0 Top Cover
BOX 1 120.00000 120.00000 120 120 20
      500.00000 1.0000 1.0000 0 0
      10.000000 9.9000 1.0000 0 0
POR 0 3 0 1 50.0000 0.00000 0.00000 0.00000
POR 1 3 0 2 50.0000 0.00000 0.00000 0.00000
NUM 2
0 5 -1 B  0 1 1 100 100
0.0000000 52.000000
58.000000 52.000000
58.000000 68.000000
0.0000000 68.000000
0.0000000 52.000000
END
0 5 -1 B  0 1 1 100 100
120.00000 46.000000
62.000000 46.000000
62.000000 74.000000
120.00000 74.000000
120.00000 46.000000
END
```

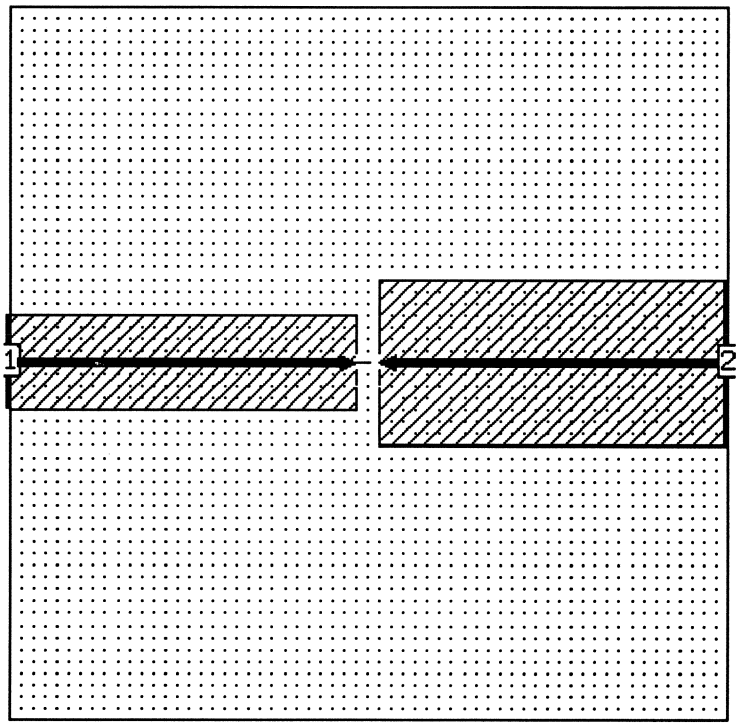

Fig. 3 (a) The nominal ".geo" file "agap0.geo" for capturing the **AGAP** and its representing structure.

```
VER 2.4a
LIC osa1.101
DAT Mon Jan 16 10:50:48 1995
LEN mil 2.5400000000e-05
SYM
REF 58.000000 58.000000 0.0000000 0.0000000 0.0000000 0.0000000 0.0000000 0.0000000
TOP 377 0 0
TON 0 Top Cover
BOX 1 120.00000 120.00000 120 120 20
      500.00000 1.0000 1.0000 0 0
      10.000000 9.9000 1.0000 0 0
POR 0 3 0 1 50.0000 0.00000 0.00000 0.00000
POR 1 3 0 2 50.0000 0.00000 0.00000 0.00000
NUM 2
0 5 -1 B  0 1 1 100 100
0.0000000 48.000000
58.000000 48.000000
58.000000 72.000000
0.0000000 72.000000
0.0000000 48.000000
END
0 5 -1 B  0 1 1 100 100
120.00000 46.000000
62.000000 46.000000
62.000000 74.000000
120.00000 74.000000
120.00000 46.000000
END
```

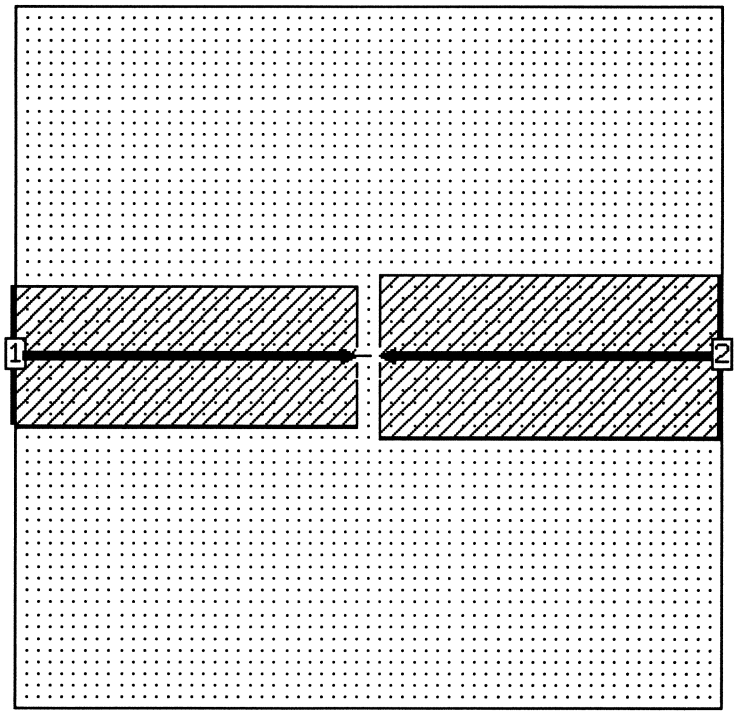

Fig. 3 (b) The ".geo" file "agap1.geo" that defines the design parameter W_1 for the **AGAP**, and its representing structure.

```
VER 2.4a
LIC osa1.101
DAT Mon Jan 16 10:52:15 1995
LEN mil 2.5400000000e-05
SYM
REF 58.000000 58.000000 0.0000000 0.0000000 0.0000000 0.0000000 0.0000000 0.0000000
TOP 377 0 0
TON 0 Top Cover
BOX 1 120.00000 128.00000 120 128 20
      500.00000 1.0000 1.0000 0 0
      10.000000 9.9000 1.0000 0 0
POR 0 3 0 1 50.0000 0.00000 0.00000 0.00000
POR 1 3 0 2 50.0000 0.00000 0.00000 0.00000
NUM 2
0 5 -1 B  0 1 1 100 100
0.0000000 56.000000
58.000000 56.000000
58.000000 72.000000
0.0000000 72.000000
0.0000000 56.000000
END
0 5 -1 B  0 1 1 100 100
120.00000 46.000000
62.000000 46.000000
62.000000 82.000000
120.00000 82.000000
120.00000 46.000000
END
```

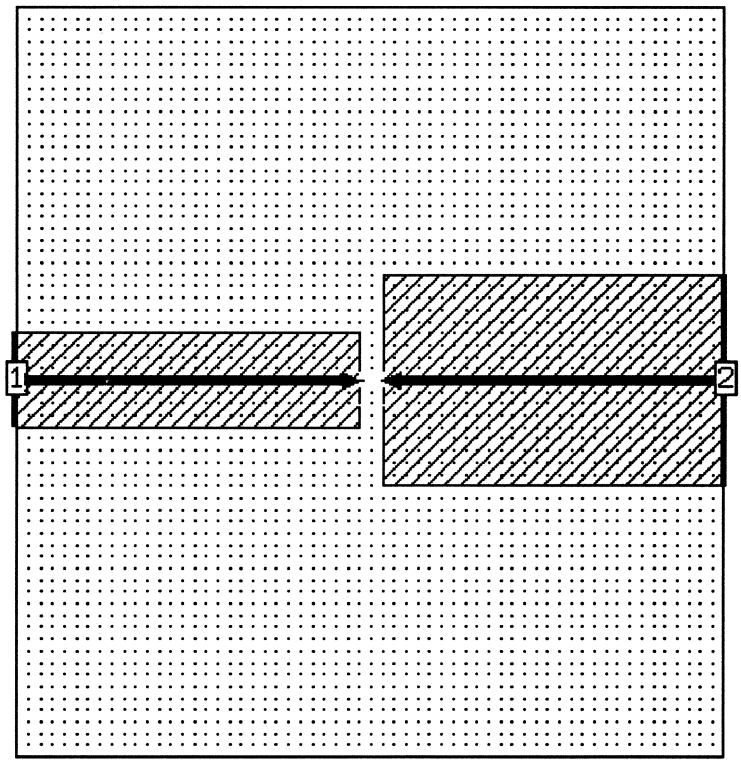

Fig. 3 (c) The ".geo" file "agap2.geo" that defines the design parameter W_2 for the **AGAP**, and its representing structure.

```
VER 2.4a
LIC osa1.101
DAT Mon Jan 16 10:53:11 1995
LEN mil 2.5400000000e-05
SYM
REF 58.000000 58.000000 0.0000000 0.0000000 0.0000000 0.0000000 0.0000000 0.0000000
TOP 377 0 0
TON 0 Top Cover
BOX 1 124.00000 120.00000 124 120 20
      500.00000 1.0000 1.0000 0 0
      10.000000 9.9000 1.0000 0 0
POR 0 3 0 1 50.0000 0.00000 0.00000 0.00000
POR 1 3 0 2 50.0000 0.00000 0.00000 0.00000
NUM 2
0 5 -1 B  0 1 1 100 100
0.0000000 52.000000
58.000000 52.000000
58.000000 68.000000
0.0000000 68.000000
0.0000000 52.000000
END
0 5 -1 B  0 1 1 100 100
124.00000 46.000000
66.000000 46.000000
66.000000 74.000000
124.00000 74.000000
124.00000 46.000000
END
```

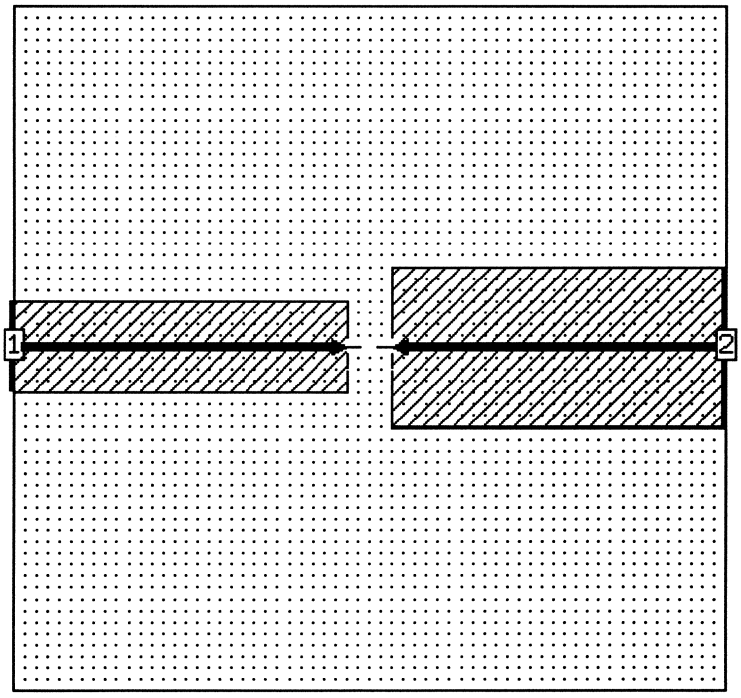

Fig. 3 (d) The ".geo" file "agap3.geo" that defines the design parameter *S* for the **AGAP**, and its representing structure.

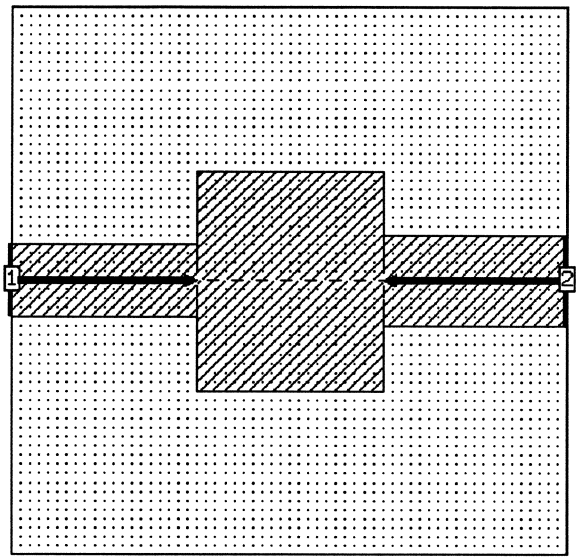

Fig. 4 (a) The nominal structure "recs0.geo" for capturing the **RECS**.

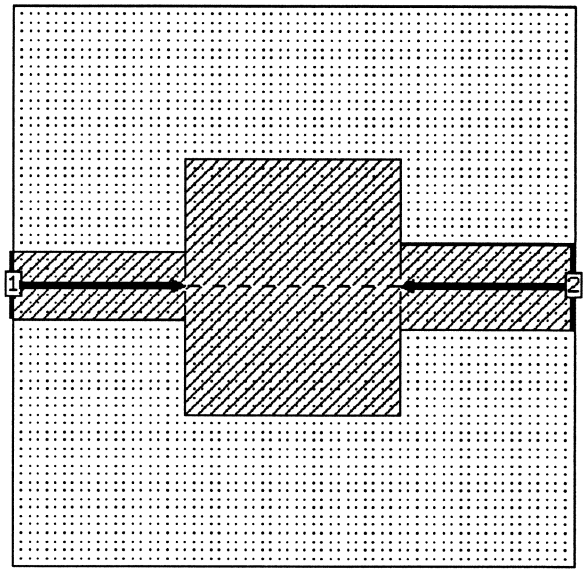

Fig. 4 (b) The structure "recs1.geo", that defines the design parameter S for the **RECS** (notice W and L change proportionally).

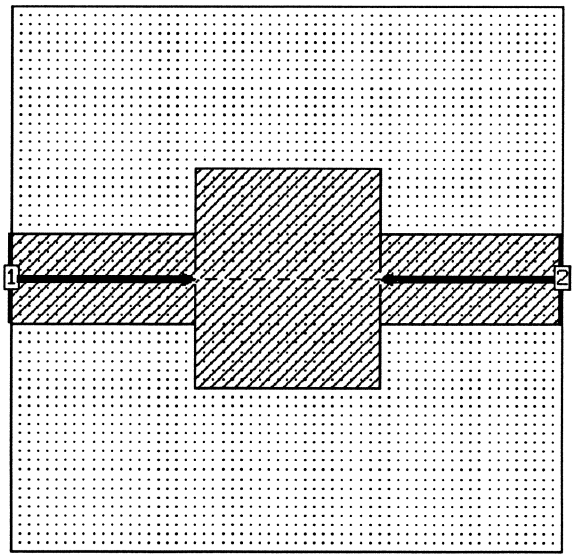

Fig. 4 (c) The structure "recs2.geo", that defines the design parameter W_1 for the **RECS**.

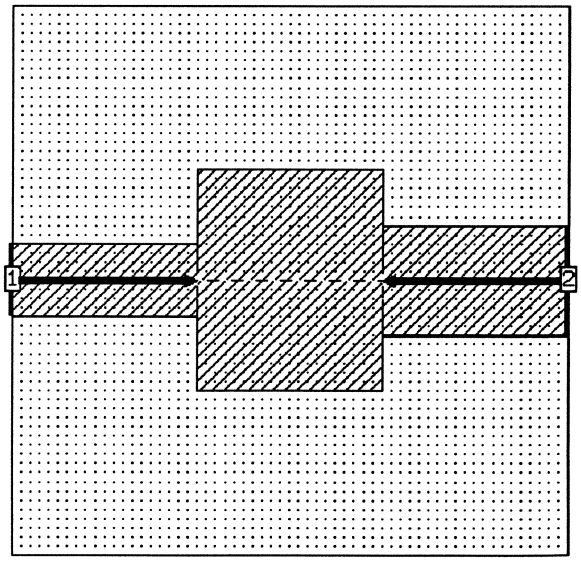

Fig. 4 (d) The structure "recs3.geo", that defines the design parameter W_2 for the **RECS**.

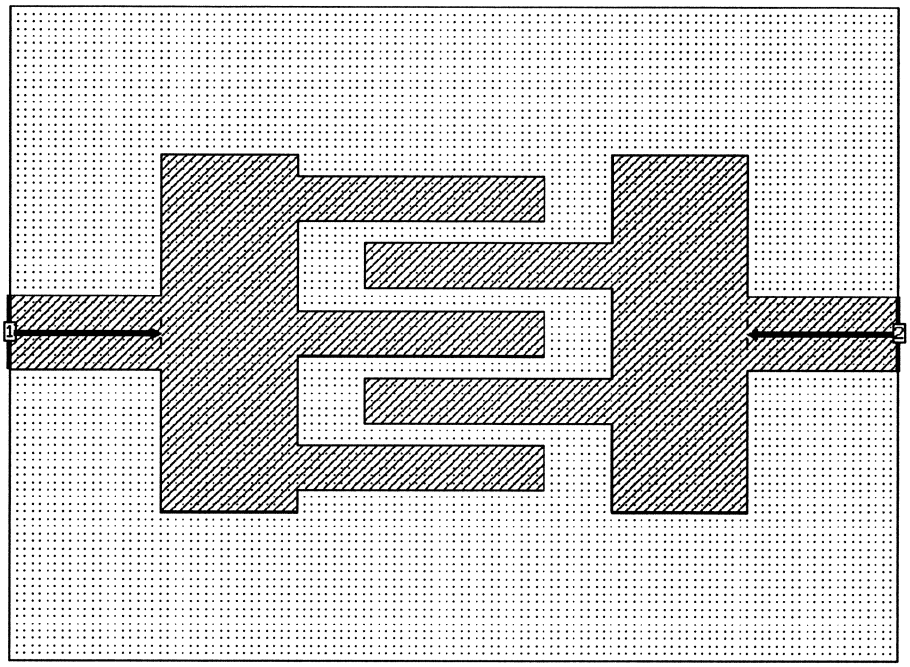

Fig. 5 (a) The nominal structure "dcap0.geo" for capturing the **DCAP** (notice two polygons are used for this structure).

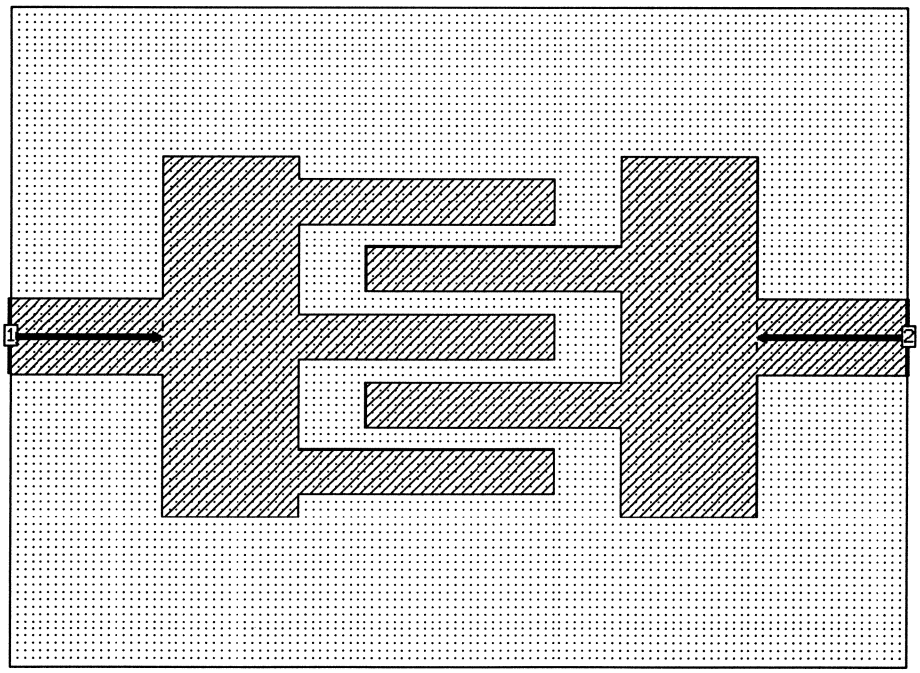

Fig. 5 (b) The structure "dcap1.geo", that defines the design parameter L for the **DCAP** (notice the distance between S and L remains constant).

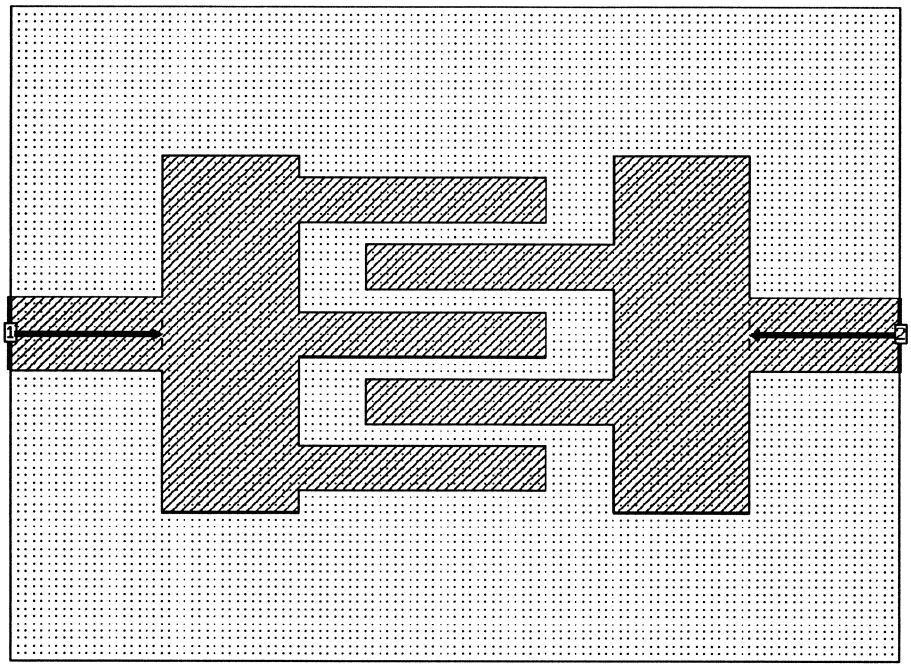

Fig. 5 (a) The nominal structure "dcap0.geo" for capturing the **DCAP** (notice two polygons are used for this structure).

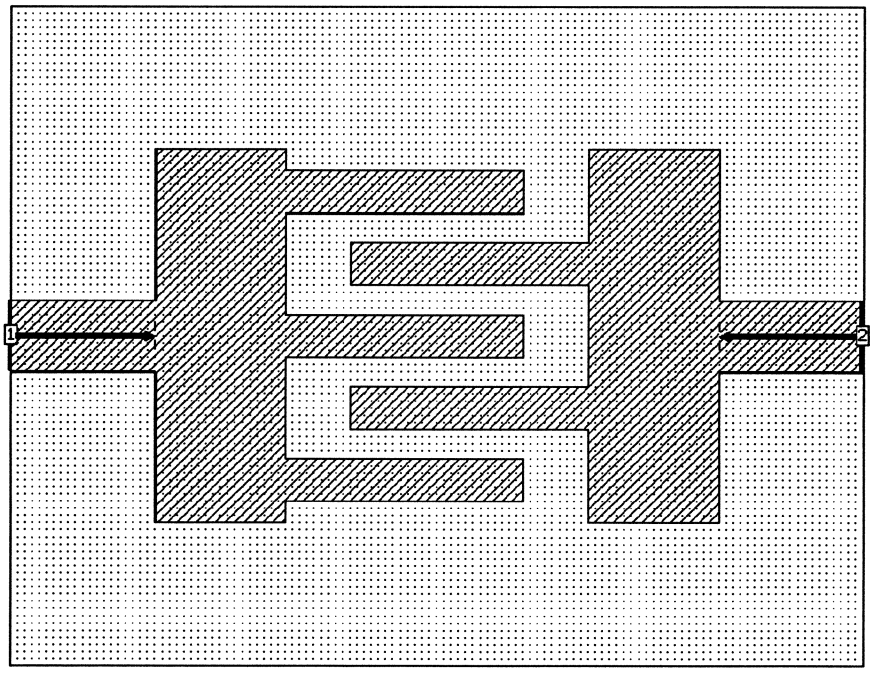

Fig. 5 (c) The structure "dcap2.geo", that defines the design parameter *G* for the **DCAP** (notice *W* changes proportionally with *G*).

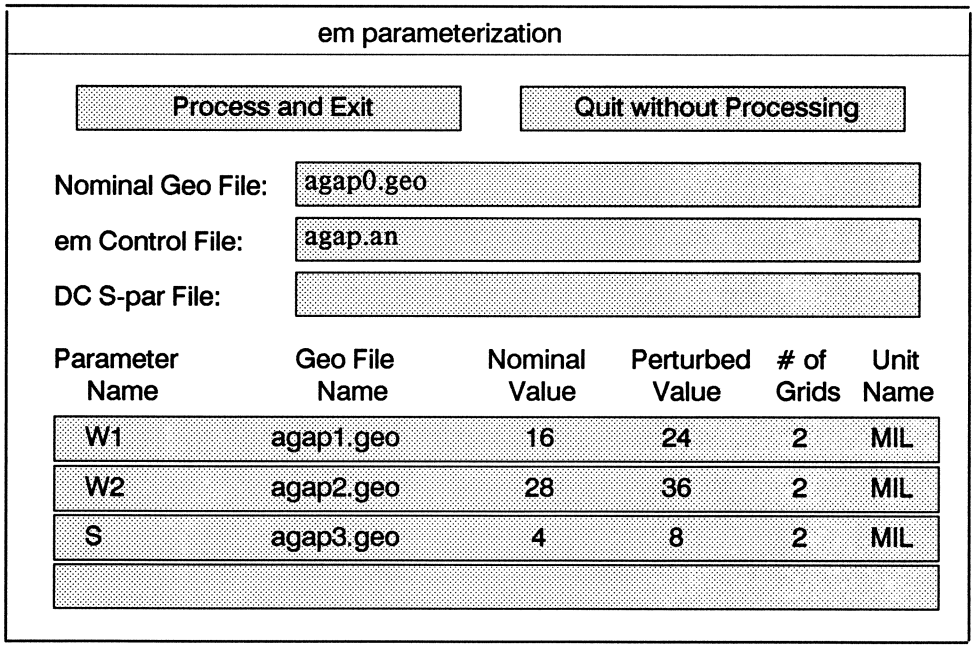

Fig. 6 ***em*** parameterization window for capturing the user defined element **AGAP**.

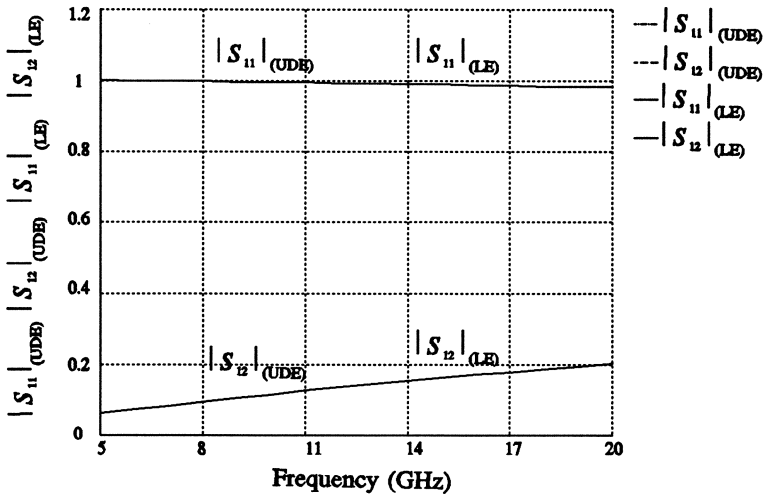

Fig. 7 (a) Response curve from the UDE approach and LE approach at the on-grid asymmetrical gap point p_1.

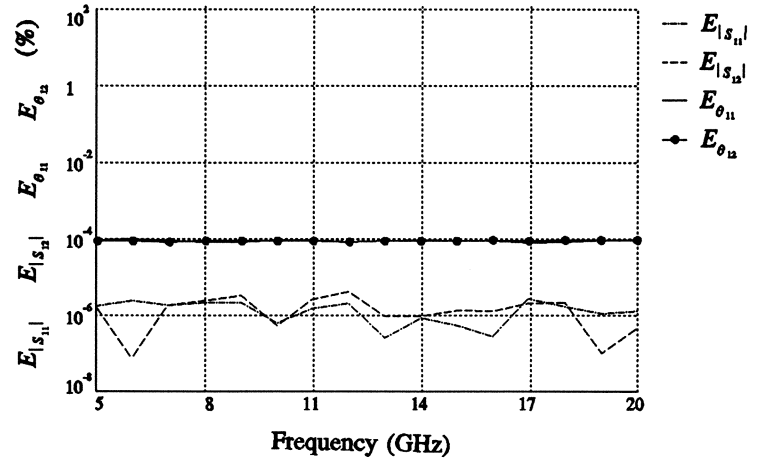

Fig. 7 (b) Error between the UDE and LE results at the on-grid asymmetrical gap point p_1.

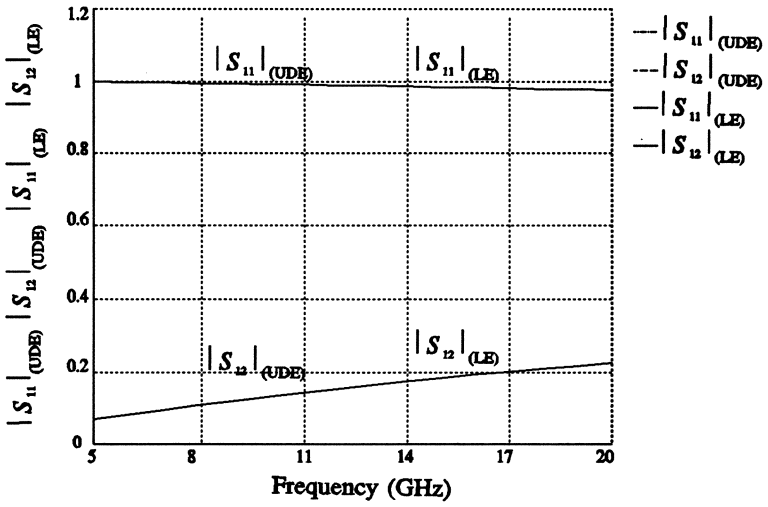

Fig. 8 (a) Response curve from the UDE approach and LE approach at the off-grid asymmetrical gap point p_2.

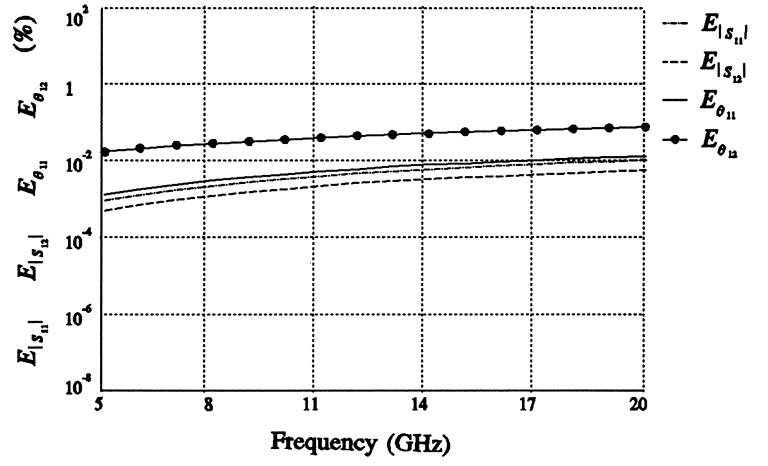

Fig. 8 (b) Error between the UDE and LE results at the off-grid asymmetrical gap point p_2.

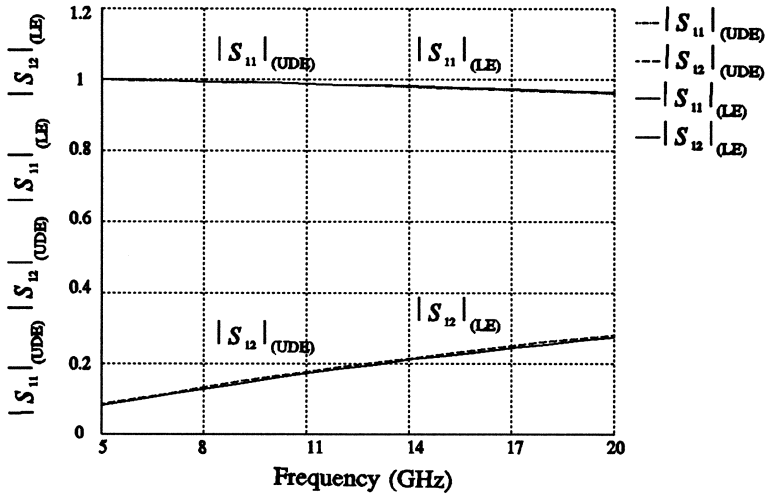

Fig. 9 (a) Response curve from the UDE approach and LE approach at the off-grid asymmetrical gap point p_3.

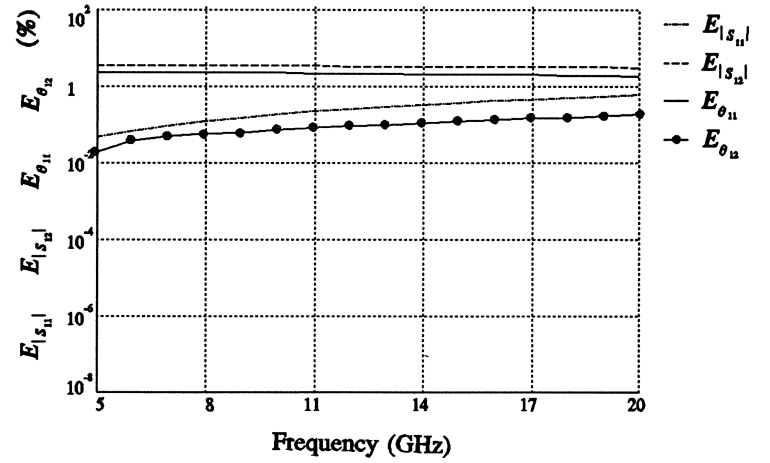

Fig. 9 (b) Error between the UDE and LE results at the off-grid asymmetrical gap point p_3.

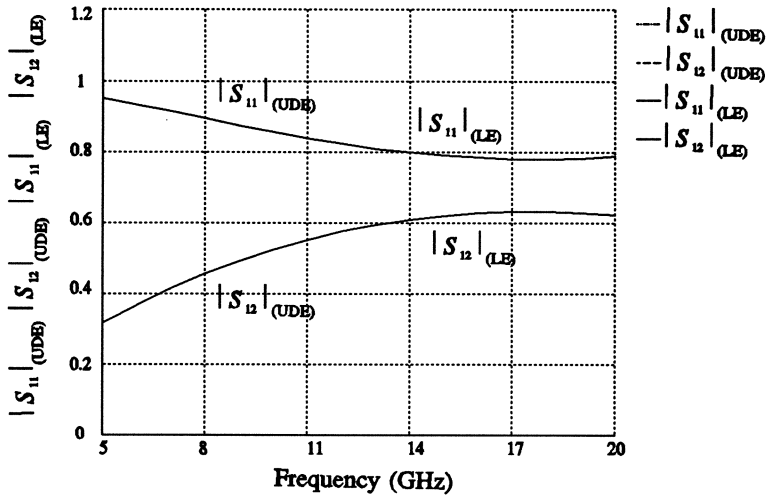

Fig. 10(a) Response curve from the UDE approach and LE approach at the mitered microstrip bend point p_4.

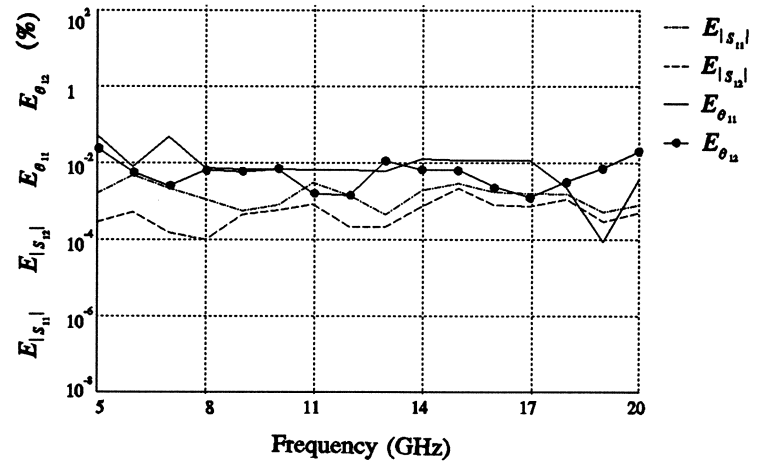

Fig. 10(b) Error between the UDE and LE results at the mitered microstrip bend point p_4.

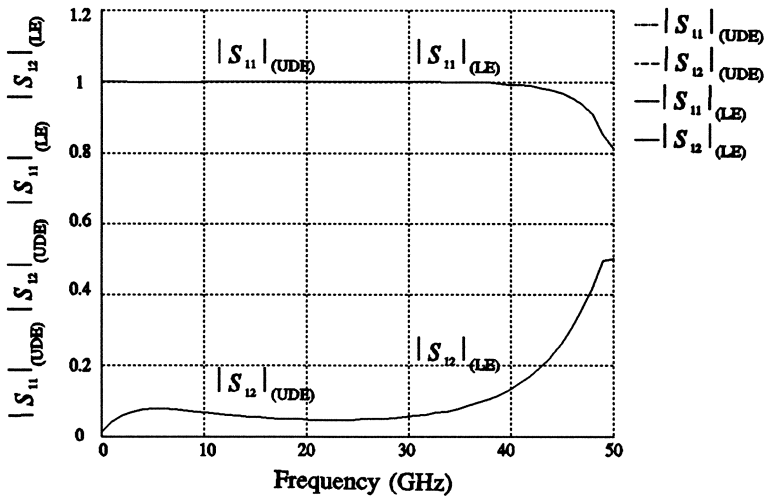

Fig. 11(a) Response curve from the UDE approach and LE approach at the microstrip double patch capacitor point p_5.

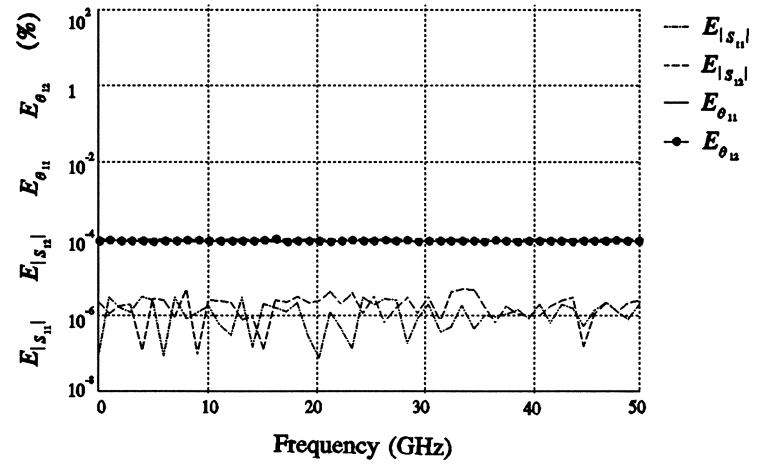

Fig. 11(b) Error between the UDE and LE results at the microstrip double patch capacitor point p_5.

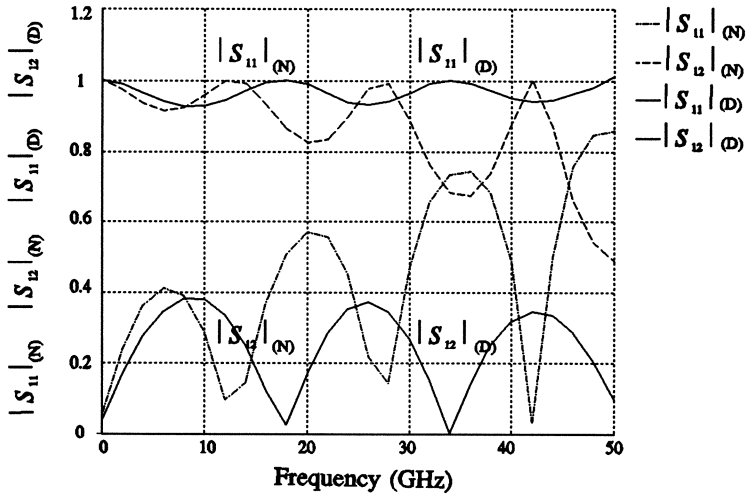

Fig. 12 De-embedding (D) and non-de-embedding (N) response curve at the microstrip line point p_6.

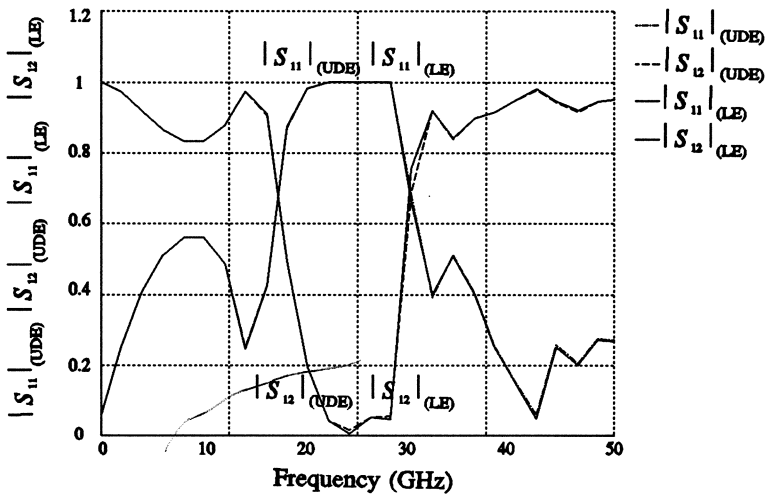

Fig. 13(a) Response curve from the UDE approach and LE approach at the asymmetrical microstrip double stub point p_7.

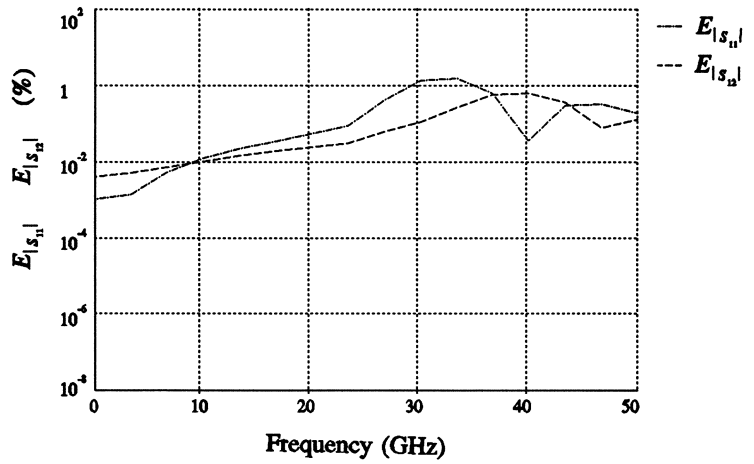

Fig. 13(b) Error between the UDE and LE results at the asymmetrical microstrip double stub point p_7.

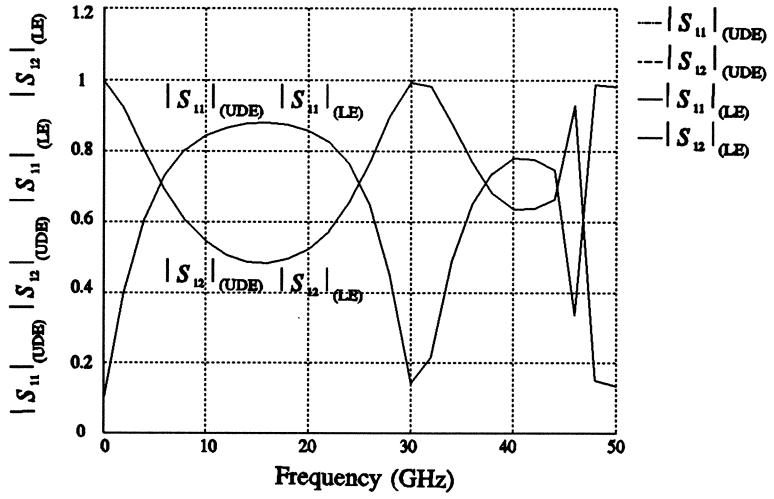

Fig. 14(h) Response curve from the UDE approach and LE approach at the microstrip rectangular structure point p_8.

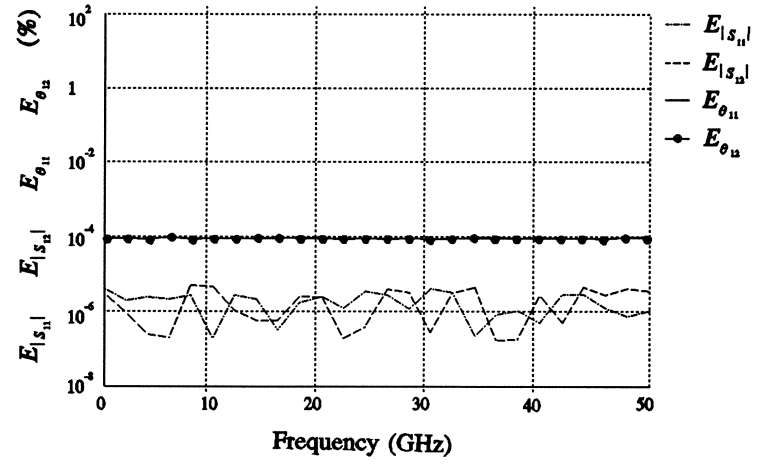

Fig. 14(b) Error between the UDE and LE results at the microstrip rectangular structure point p_8.

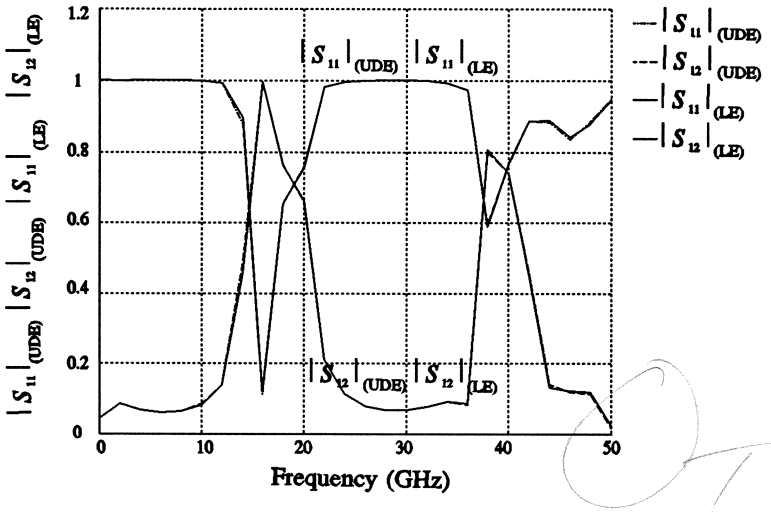

Fig. 15(a) Response curve from the UDE approach and LE approach at the microstrip interdigital capacitor point p_9.

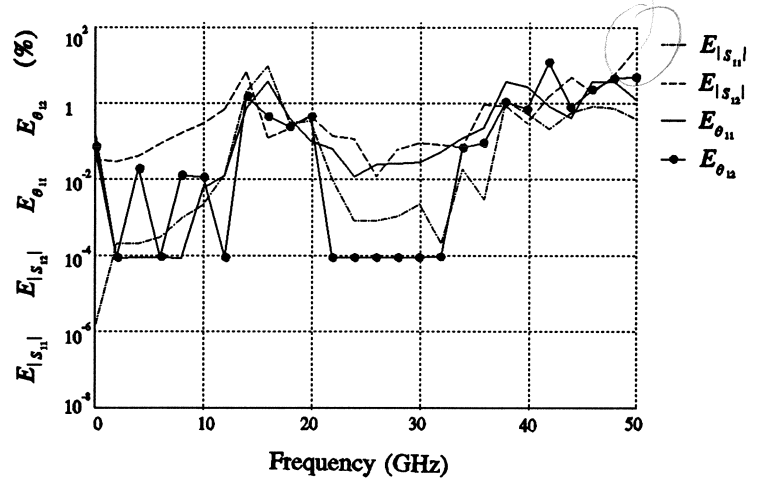

Fig. 15(b) Error between the UDE and LE results at the microstrip interdigital capacitor point p_9.

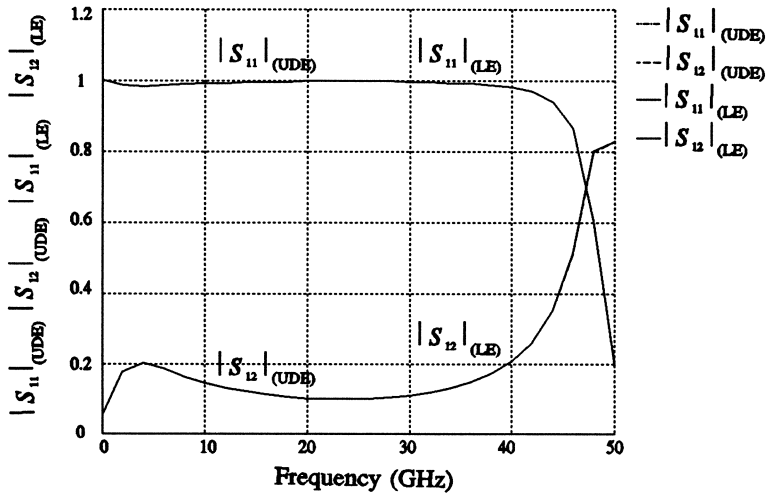

Fig. 16(a) Response curve from the UDE approach and LE approach at the microstrip overlay patch capacitor point p_{10}.

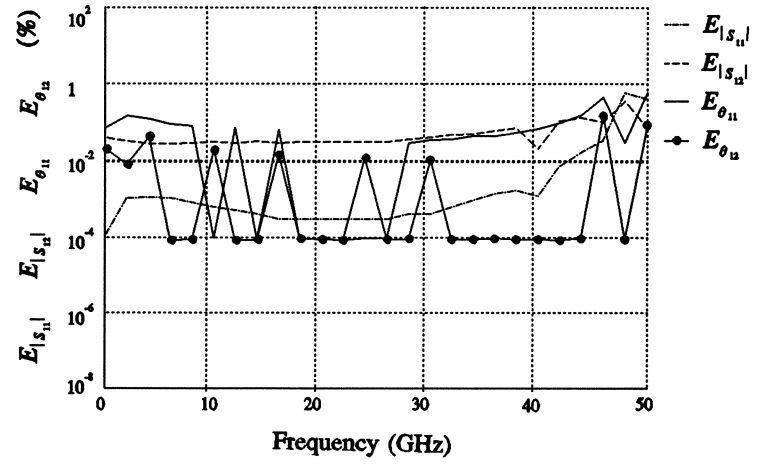

Fig. 16(b) Error between the UDE and LE results at the microstrip overlay patch capacitor point p_{10}.

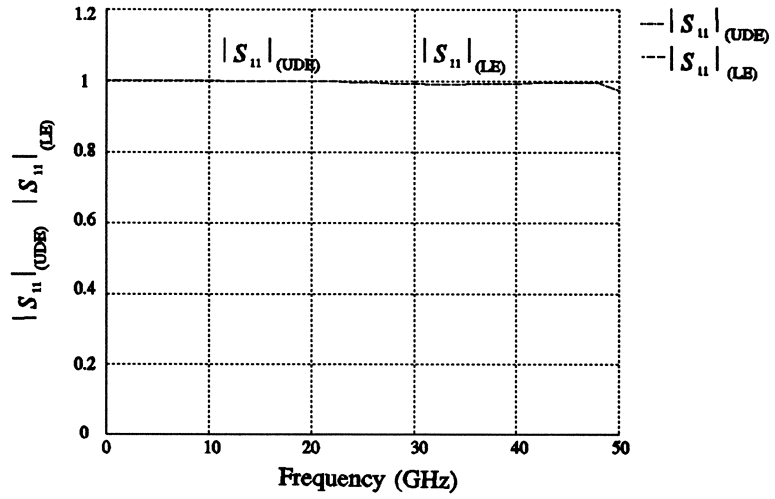

Fig. 17(a) Response curve from the UDE approach and LE approach at the lossy microstrip open stub point p_{11}.

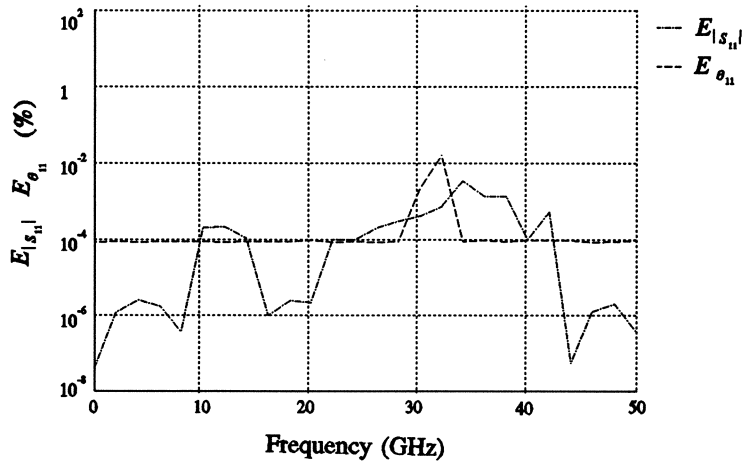

Fig. 17(b) Error between the UDE and LE results at the microstrip open stub point p_{11}.

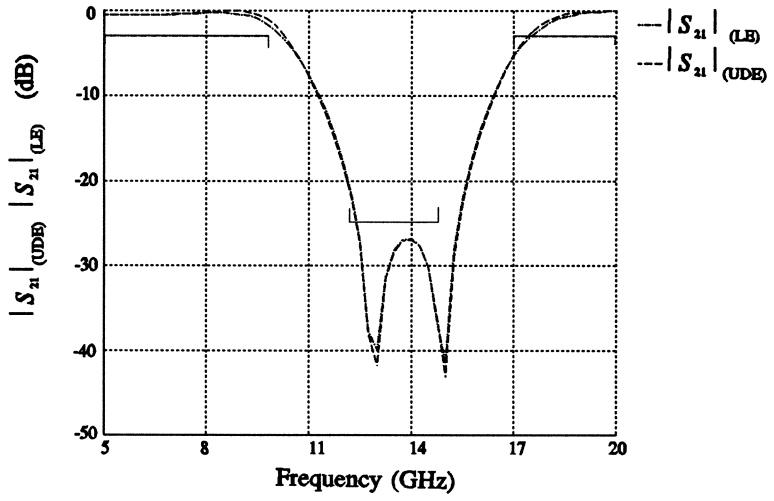

Fig. 18(b) Filter response $|S_{21}|$ simulation from the UDE approach and LE approach at point p_s before optimization.

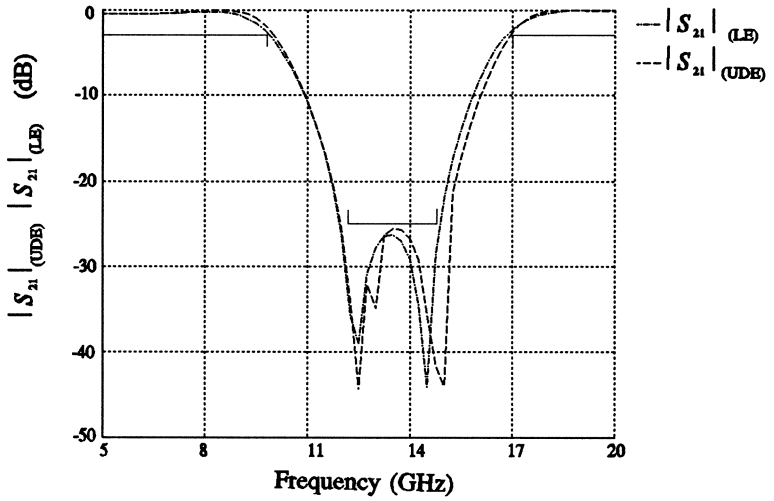

Fig. 18(b) Filter response $|S_{21}|$ simulation at the UDE optimum and the LE optimum.

Appendix A

1. Circuit file comparing the UDE and LE simulation results for an on-grid asymmetrical microstrip gap.

```
Model

#include "agap.inc"
#include "/home/spicy/nancy/em/em_agap.inc"

   AGAP  1 2 0  W1=16mil W2=28mil S=4mil H=10mil;
   PORTS 1 0 2 0;

   EM_AGAP  3 4 0  INDEX=17 W1=16mil W2=28mil S=4mil H=10mil EPSR=9.9
                   XCELL=2mil YCELL=2mil FMIN=5ghz FMAX=20ghz FSTEP=1.0ghz
                   UNIT=0 LEFT=5.8 RIGHT=5.8 TOP=4.6 BOTTOM=4.6;
   PORTS 3 0 4 0;

   CIRCUIT;

   EMS11=(ABS(MS11-MS33))/(ABS(MS11))*100;
   EMS12=(ABS(MS12-MS34))/(ABS(MS12))*100;
   EPS11=(ABS(PS11-PS33))/(ABS(PS11))*100;
   EPS12=(ABS(PS12-PS34))/(ABS(PS12))*100;

end

Sweep

   AC: freq: from 5ghz to 20ghz step=1.0ghz  MS11 MS12 MS33 MS34;

end
```

Geometry file generated in the UDE approach

```
VER 2.4a
LIC osa1.101
DAT Mon Jan 16 10:48:51 1995
LEN mil 2.5400000000e-05
SYM
REF 58.000000 58.000000 0.0000000 0.0000000 0.0000000 0.0000000 0.0000000 0.0000000
TOP 377 0 0
TON 0 Top Cover
BOX 1 120      120       120 120 20
      500.00000 1.0000 1.0000 0 0
      10      9.9000 1.0000 0 0
POR 0 3 0 1 50.0000 0.00000 0.00000 0.00000
POR 1 3 0 2 50.0000 0.00000 0.00000 0.00000
NUM 2
0 5 -1 B  0 1 1 100 100          ! Polygon 1
0.0000000 52
58.000000 52
58.000000 68
0.0000000 68
0.0000000 52
END
0 5 -1 B  0 1 1 100 100          ! Polygon 2
120      46.000000
62      46.000000
62      74
120      74
120      46.000000
```

```
END
```

Geometry file generated in the LE approach

```
VER 2.3a
LIC your.lic
LEN  mil 2.540000E-05
TOP 377 0 0
TON 0 Top Cover
SYM
BOX 1   1.2000000E+02 1.2000000E+02 120 120 20
  500.000000 1.0  1.0  0  0
  10.000000 9.900000  1.000000  0.000000  0.000000
POR 0 0 0 1 50.0  0.0  0.0  0.0
POR 1 2 0 2 50.0  0.0  0.0  0.0
REF   5.8000000E+01   5.8000000E+01   0.0000000E+00   0.0000000E+00
NUM 2
0 5 -1 B  0 1 1 100 100         ! Polygon 1
  0.0000000E+00    5.2000000E+01
  0.0000000E+00    6.8000000E+01
  5.8000000E+01    6.8000000E+01
  5.8000000E+01    5.2000000E+01
  0.0000000E+00    5.2000000E+01
END
0 5 -1 B  0 1 1 100 100         ! Polygon 2
  6.2000000E+01    4.6000000E+01
  6.2000000E+01    7.4000000E+01
  1.2000000E+02    7.4000000E+01
  1.2000000E+02    4.6000000E+01
  6.2000000E+01    4.6000000E+01
END
```

Appendix B

1. File "agap.inc".

```
! User-Parameterized Struture: agap

ELEMENT  agap  1 2 0
      INDEX=8 MODEL=3
      W1=16MIL W2=28MIL S=4MIL H=10MIL {
   N_Pars = 4;
   Pars[4] = [(W1 / 1MIL) (W2 / 1MIL) (S / 1MIL) (H / 1MIL) ];
   Grids[4] = [4 4 2 0.5 ];
   Delta[4] = [1 1 1 1];
   char DBS[]="agap";
   char gem_file[] = "
@SETUP INFORMATION
   NOMINAL GEO FILE agap0.geo
   EM CONTROL FILE agap.an
   Parameter      Geo File        Nominal  Perturbed  # of   Unit
     Name           Name          Value     Value    Grids  Name
    W1          agap1.geo            16        24      2    MIL
    W2          agap2.geo            28        36      2    MIL
    S           agap3.geo             4         8      2    MIL
    H           agap4.geo            10        11      2    MIL
@SETUP END
@GEM PARAMETERS: 4 17
@GEM NOMINAL: 16 28 4 10
@GEM COE:
 52 -0.5 0.5 0 0
 52 -0.5 0.5 0 0
 68 0.5 0.5 0 0
 68 0.5 0.5 0 0
 52 -0.5 0.5 0 0
 120 0 1 0 0
 120 0 1 0 0
 74 0 1 0 0
 74 0 1 0 0
 120 0 0 1 0
 120 0 0 1 0
 120 0 0 1 0
 62 0 0 1 0
 62 0 0 1 0
 120 0 0 1 0
 120 0 0 1 0
 10 0 0 0 1

@GEM CTL
VER 2.4a
GHz
FRE  5.00000000  20.000000  1.0
@GEM GEO
VER 2.4a
LIC osa1.101
DAT Mon Jan 16 10:48:51 1995
LEN mil 2.5400000000e-05
SYM
REF 58.000000 58.000000 0.0000000 0.0000000 0.0000000 0.0000000 0.0000000 0.0000000
TOP 377 0 0
TON 0 Top Cover
BOX 1 @V10@     @V6@      @V11@ @V7@ 20
      500.00000 1.0000 1.0000 0 0
      @V17@     9.9000 1.0000 0 0
POR 0 3 0 1 50.0000 0.00000 0.00000 0.00000
POR 1 3 0 2 50.0000 0.00000 0.00000 0.00000
NUM 2
0 5 -1 B  0 1 1 100 100
```

```
0.0000000 @V1@
58.000000 @V2@
58.000000 @V3@
0.0000000 @V4@
0.0000000 @V5@
END
0 5 -1 B  0 1 1 100 100
@V12@     46.000000
@V13@     46.000000
@V14@     @V8@
@V15@     @V9@
@V16@     46.000000
END
";

   N_FREQ=16;
   N_OUT=9;
   char Simulator[] = "em -Qdm";
   SAVE_DBS=1;
   Datapipe: COM FILE="empipe20" PRO=749 N_INPUT=(7+3*N_Pars)
             INPUT=(INDEX, MODEL, SAVE_DBS, DBS, Pars, GEM_file,
                    Grids, Delta, Simulator, 0)
             N_OUTPUT=(N_FREQ * N_OUT)  OUTPUT=(SMP[N_FREQ,N_OUT]);

   SPORT 1 2 0 FMP=SMP;
};
```

2. Parameterization portion of the "bendm.inc" file.

```
ELEMENT  bendm  1 2 0
      INDEX=1 MODEL=3
      W1=32MIL W2=32MIL L1=22MIL L2=22MIL EPSR=9.8 {
   N_Pars = 5;
   Pars[5] = [(W1 / 1MIL) (W2 / 1MIL) (L1 / 1MIL) (L2 / 1MIL) EPSR ];
   Grids[5] = [2 2 2 2 0.1 ];
   Delta[5] = [1 1 1 1 1];
   char DBS[]="bendm";
   char gem_file[] = "
@SETUP INFORMATION
   NOMINAL GEO FILE bendm0.geo
   EM CONTROL FILE bendm.an
   Parameter      Geo File        Nominal  Perturbed  # of   Unit
     Name           Name           Value     Value    Grids  Name
    W1         bendm1.geo           32        34       1    MIL
    W2         bendm2.geo           32        36       2    MIL
    L1         bendm3.geo           22        24       1    MIL
    L2         bendm4.geo           22        26       2    MIL
    EPSR       bendm5.geo          9.8       9.9       1    none
@SETUP END
```

3. Parameterization portion of the "dpcap.inc" file.

```
ELEMENT  dpcap  1 2 0
      INDEX=1 MODEL=3
      L1=24MIL L2=28MIL S=4MIL W1=20MIL W2=60MIL W3=16MIL {
   N_Pars = 6;
   Pars[6] = [(L1 / 1MIL) (L2 / 1MIL) (S / 1MIL) (W1 / 1MIL) (W2 / 1MIL) (W3 / 1MIL) ];
   Grids[6] = [2 2 2 4 4 4 ];
   Delta[6] = [1 1 1 1 1 1];
   char DBS[]="dpcap";
   char gem_file[] = "
@SETUP INFORMATION
   NOMINAL GEO FILE dpcap0.geo
   EM CONTROL FILE dpcap.an
```

```
   Parameter      Geo File        Nominal  Perturbed  # of   Unit
     Name          Name           Value     Value    Grids  Name
    L1          dpcap1.geo          24        26       1    MIL
    L2          dpcap2.geo          28        30       1    MIL
    S           dpcap3.geo           4         6       1    MIL
    W1          dpcap4.geo          20        24       1    MIL
    W2          dpcap5.geo          60        64       1    MIL
    W3          dpcap6.geo          16        20       1    MIL
@SETUP END
```

4. Parameterization portion of the "ml.inc" file.

```
ELEMENT  ml  1 2 0
      INDEX=1 MODEL=3
      L=120MIL W=20MIL {
   N_Pars = 2;
   Pars[2] = [(L / 1MIL) (W / 1MIL) ];
   Grids[2] = [2 4 ];
   Delta[2] = [1 1];
   char DBS[]="ml";
   char gem_file[] = "
@SETUP INFORMATION
   NOMINAL GEO FILE ml0.geo
   EM CONTROL FILE ml.an
   Parameter      Geo File        Nominal  Perturbed  # of   Unit
     Name          Name           Value     Value    Grids  Name
    L          ml1.geo             120       122       1    MIL
    W          ml2.geo              20        24       1    MIL
@SETUP END
```

5. Parameterization portion of the "dstb.inc" file.

```
ELEMENT  dstb  1 2 0
      INDEX=1 MODEL=3
      W2=20MIL W3=16MIL L1=34MIL L2=40MIL L3=38MIL {
   N_Pars = 5;
   Pars[5] = [(W2 / 1MIL) (W3 / 1MIL) (L1 / 1MIL) (L2 / 1MIL) (L3 / 1MIL) ];
   Grids[5] = [2 2 2 4 4 ];
   Delta[5] = [1 1 1 1 1];
   char DBS[]="dstb";
   char gem_file[] = "
@SETUP INFORMATION
   NOMINAL GEO FILE dstb0.geo
   EM CONTROL FILE dstb.an
   Parameter      Geo File        Nominal  Perturbed  # of   Unit
     Name          Name           Value     Value    Grids  Name
    W2          dstb1.geo           20        22       1    MIL
    W3          dstb2.geo           16        18       1    MIL
    L1          dstb3.geo           34        36       1    MIL
    L2          dstb4.geo           40        44       1    MIL
    L3          dstb5.geo           38        42       1    MIL
@SETUP END
```

6. Parameterization portion of the "recs.inc" file.

```
ELEMENT  recs  1 2 0
      INDEX=1 MODEL=3
      S=4 W1=16MIL W3=20MIL {
   N_Pars = 3;
   Pars[3] = [S (W1 / 1MIL) (W3 / 1MIL) ];
   Grids[3] = [1 4 4 ];
```

```
   Delta[3] = [1 1 1];
   char DBS[]="recs";
   char gem_file[] = "
@SETUP INFORMATION
   NOMINAL GEO FILE recs0.geo
   EM CONTROL FILE recs.an
   Parameter      Geo File        Nominal  Perturbed  # of   Unit
     Name           Name           Value     Value    Grids  Name
    S          recs1.geo             4         5       1    none
    W1         recs2.geo            16        20       1    MIL
    W3         recs3.geo            20        24       1    MIL
@SETUP END
```

7. Parameterization portion of the "dcap.inc" file.

```
ELEMENT  dcap  1 2 0
      INDEX=1 MODEL=3
      L=66MIL G=6MIL {
   N_Pars = 2;
   Pars[2] = [(L / 1MIL) (G / 1MIL) ];
   Grids[2] = [2 2 ];
   Delta[2] = [1 1];
   char DBS[]="dcap";
   char gem_file[] = "
@SETUP INFORMATION
   NOMINAL GEO FILE dcap0.geo
   EM CONTROL FILE dcap.an
   Parameter      Geo File        Nominal  Perturbed  # of   Unit
     Name           Name           Value     Value    Grids  Name
    L          dcap1.geo            66        68       1    MIL
    G          dcap2.geo             6         8       1    MIL
@SETUP END
```

8. Parameterization portion of the "odpc.inc" file.

```
ELEMENT  odpc  1 2 0
      INDEX=1 MODEL=3
      W1=16MIL W2=48MIL W3=36MIL L1=22MIL L3=24MIL S=4MIL {
   N_Pars = 6;
   Pars[6] = [(W1 / 1MIL) (W2 / 1MIL) (W3 / 1MIL) (L1 / 1MIL) (L3 / 1MIL) (S / 1MIL) ];
   Grids[6] = [4 4 4 2 4 4 ];
   Delta[6] = [1 1 1 1 1 1];
   char DBS[]="odpc";
   char gem_file[] = "
@SETUP INFORMATION
   NOMINAL GEO FILE odpc0.geo
   EM CONTROL FILE odpc.an
   Parameter      Geo File        Nominal  Perturbed  # of   Unit
     Name           Name           Value     Value    Grids  Name
    W1         odpc1.geo            16        20       1    MIL
    W2         odpc2.geo            48        52       1    MIL
    W3         odpc3.geo            36        40       1    MIL
    L1         odpc4.geo            22        24       1    MIL
    L3         odpc5.geo            24        28       1    MIL
    S          odpc6.geo             4         8       1    MIL
@SETUP END
```

9. Parameterization portion of the "ope.inc" file.

```
ELEMENT  ope  1 0
      INDEX=1 MODEL=3
```

```
      W=20MIL L=60MIL {
   N_Pars = 2;
   Pars[2] = [(W / 1MIL) (L / 1MIL) ];
   Grids[2] = [4 2 ];
   Delta[2] = [1 1];
   char DBS[]="ope";
   char gem_file[] = "
@SETUP INFORMATION
   NOMINAL GEO FILE ope0.geo
   EM CONTROL FILE ope.an
   Parameter      Geo File        Nominal  Perturbed  # of   Unit
     Name           Name           Value     Value    Grids  Name
    W          ope1.geo              20        24       1    MIL
    L          ope2.geo              60        62       1    MIL
@SETUP END
```

10. Parameterization portion of the "fdst.inc" file.

```
ELEMENT  fdstll  1 2 0
      INDEX=1 MODEL=3
      W=18MIL L1=44MIL L2=36MIL L3=40MIL S1=22MIL S2=20MIL {
   N_Pars = 6;
   Pars[6] = [(W / 1MIL) (L1 / 1MIL) (L2 / 1MIL) (L3 / 1MIL) (S1 / 1MIL) (S2 / 1MIL) ];
   Grids[6] = [2 2 4 4 2 2 ];
   Delta[6] = [1 1 1 1 1 1];
   char DBS[]="fdst";
   char gem_file[] = "
@SETUP INFORMATION
   NOMINAL GEO FILE fdst0.geo
   EM CONTROL FILE fdst.an
   Parameter      Geo File        Nominal  Perturbed  # of   Unit
     Name           Name           Value     Value    Grids  Name
    W          fdst1.geo             18        20       1    MIL
    L1         fdst2.geo             44        46       1    MIL
    L2         fdst3.geo             36        40       1    MIL
    L3         fdst4.geo             40        44       1    MIL
    S1         fdst5.geo             22        24       1    MIL
    S2         fdst6.geo             20        22       1    MIL
@SETUP END
```